AMERICAN MUSEUM NOVITATES

Number 3878, 44 pp. April 14, 2017

New material of Eocene Helaletidae (Perissodactyla, Tapiroidea) from the Irdin Manha Formation of the Erlian Basin, Inner Mongolia, China and comments on Related Localities of the Huheboerhe Area

BIN BAI,[1, 2] YUAN-QING WANG,[1, 3] FANG-YUAN MAO,[1] AND JIN MENG[4]

ABSTRACT

Perissodactyls first appeared at the beginning of the early Eocene and reached their highest diversity, dominating contemporaneous mammalian faunas in species richness during the middle Eocene. Tapiroidea is an important perissodactyl group that includes earliest-Eocene forms, such as *Orientolophus* as well as extant taxa (such as *Tapirus*), that preserves numerous plesiomorphic characters. Because tapiroids were widely distributed in North America and Asia in the middle Eocene, they have played an important role in biostratigraphically defining middle Eocene North American Land Mammal Ages (NALMA) and Asian Land Mammal Ages (ALMA), respectively, as well as in biostratigraphic correlation between the two continents. Here we report a new cranial specimen of middle Eocene helaletid *Paracolodon fissus* and a maxilla of *Desmatotherium mongoliense* from the middle Eocene Irdin Manha Formation of the Erlian Basin, Inner Mongolia, China. *Paracolodon fissus* was previously assigned to *Desmatotherium*, *Helaletes*, or *Colodon*, whereas *D. mongoliense* was assigned to *Helaletes* or *Irdinolophus* by different authors. Based on the new material described in this report, we are able to clarify the affinities and phylogenetic position of these species according

[1] Key Laboratory of Vertebrate Evolution and Human Origins of Chinese Academy of Sciences, Institute of Vertebrate Paleontology and Paleoanthropology, Chinese Academy of Sciences, Beijing.
[2] State Key Laboratory of Palaeobiology and Stratigraphy, Nanjing Institute of Geology and Palaeontology, Chinese Academy of Sciences, Nanjing.
[3] College of Earth Sciences, University of Chinese Academy of Sciences, Beijing.
[4] Division of Paleontology, American Museum of Natural History, New York.

 ISSN 0003-0082

to morphological comparison and phylogenetic analyses. We maintain the genus *Paracolodon* for *P. inceptus* and *P. fissus* from Asia and reassign *mongoliense* to *Desmatotherium*. Fossils of perissodactyls and other groups from the Irdin Manha Formation favor correlation of the Irdinmanhan ALMA with the early and middle Uintan NALMA (Ui1-Ui2). Through our field investigation, we also clarified that the localities "7 miles southwest" and "10 miles southwest" of Camp Margetts, originally used by the American Museum of Natural History's Central Asiatic Expedition (CAE), correspond to the localities currently known as Huheboerhe and Changanboerhe, respectively.

INTRODUCTION

The tapiroid perissodactyls have a great diversity in the Eocene, and are common in the Eocene deposits of the northern continents (Hooker, 1989; 2005). Tapiroidea is traditionally composed of Isectolophidae, Helaletidae, Lophialetidae, Deperetellidae, Tapiridae, and Lophiodontidae (McKenna and Bell, 1997). Lophialetidae and Deperetellidae are endemic Asian groups (Radinsky, 1965a), whereas Lophiodontidae is restricted in Europe (Holbrook, 2009). Helaletidae is distributed in both Asia and North America, and thus plays an important role in the intercontinental correlation of faunal ages (Radinsky, 1963; Radinsky, 1965a). Despite a long history of research, the phylogenetic relationships among different families of tapiroids remain obscure. Recent studies suggest that Isectolophidae is not a monophyletic group and that Lophiodontidae is probably more closely related to Chalicotherioidea (Holbrook et al., 2004; Hooker and Dashzeveg, 2004; Bai et al., 2014).

Helaletidae is a basal group of Tapiroidea, ranging from early Eocene to Oligocene (Radinsky, 1963; Colbert and Schoch, 1998). According to McKenna and Bell (1997), Helaletidae consists of six genera: *Cymbalophus*, *Heptodon*, *Selenaletes*, *Helaletes*, *Colodon*, and *Plesiocolopirus*, whereas Radinsky (1963) also included *Dilophodon* in the family. Of these genera, *Cymbalophus* was considered as a basal tapiromorph (Hooker, 1984) or equoid (Hooker and Dashzeveg, 2004; Hooker, 2010) and should be excluded from Helaletidae. In his comprehensive review of North American Paleogene Tapiroidea, Radinsky (1963) synonymized the genera *Desmatotherium* and *Heteraletes* with *Helaletes* and *Dilophodon*, respectively. However, some authors still supported the validity of *Desmatotherium* and *Heteraletes* (Schoch, 1984; Schoch, 1989; Colbert and Schoch, 1998). Recently, the primitive tapiromorph *Cambaylophus* and helaletid *Vastanolophus* were reported from India, and several authors argue that at least tapiroid perissodactyls originated in India (Cooper et al., 2014; Rose et al., 2014; Kapur and Bajpai, 2015; Smith et al., 2015).

The first Asian helaletid was reported by Borissiak (1918) as *Colodon*? *orientalis* from the Turgai region, Kazakhstan. Osborn (1923) and Matthew and Granger (1925b) described *Desmatotherium mongoliense* and *D. fissum* from the Erlian Basin, Inner Mongolia, but Radinsky (1965a) assigned both species to *Helaletes* and noticed some of their similarities with *Colodon*. Matthew and Granger (1925a) also named *Colodon inceptus* and *Paracolodon curtus* from Ergilin Dzo (Ardyn Obo), Mongolia, but Radinsky (1965a) considered the latter a junior synonym of the former. In reporting additional material of helaletids from Ergilin Dzo and Mergen, Mongolia, Dashzeveg and Hooker (1997) suggested a close affinity between "*Helaletes* " *fissus* and *Colodon inceptus* and eventually assigned the species *"Helaletes " fissus* as *Colodon fissus*.

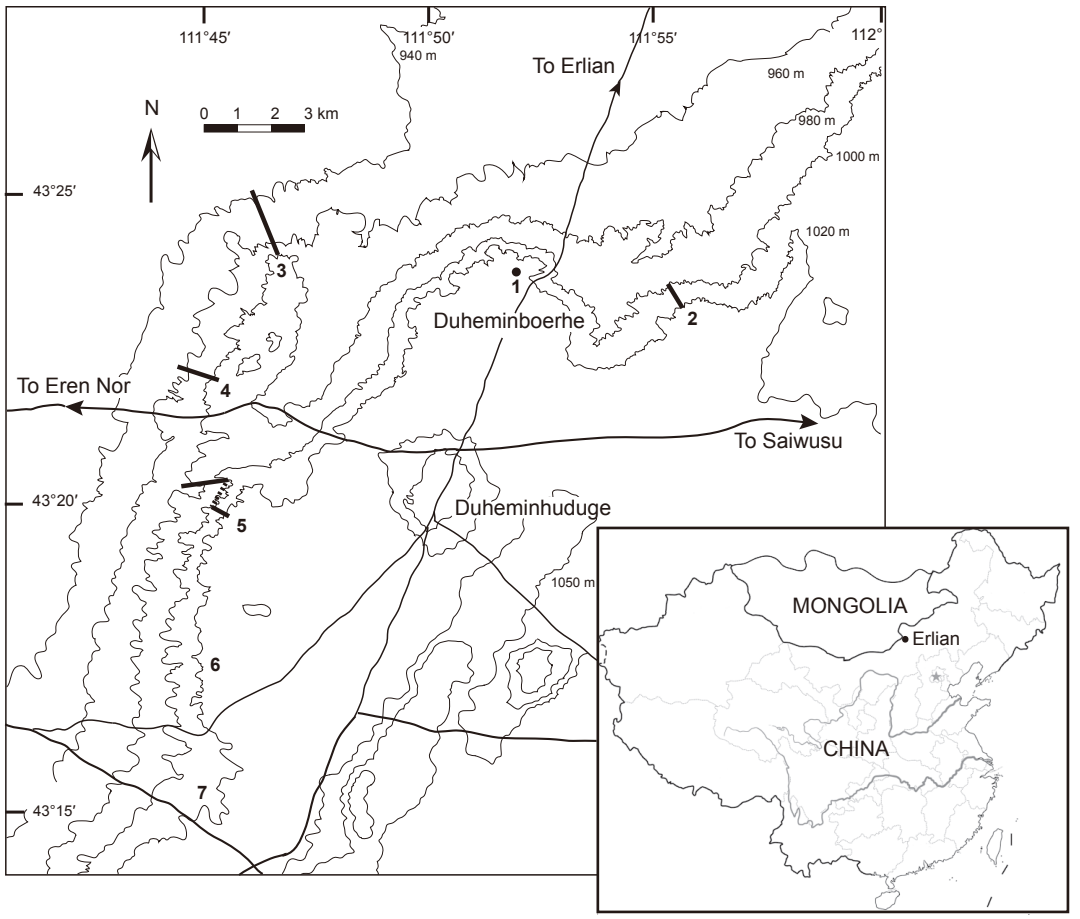

FIG. 1. Topographic map of the Huheboerhe area (modified from Meng et al., 2007: fig. 1). **1,** presumed location of Camp Margetts; **2,** Daoteyin Obo (5 miles east of Camp Margetts); **3,** Nuhetingboerhe (6 miles west of Camp Margetts); **4,** Wulanboerhe; **5,** Huheboerhe (7 miles west and southwest [235°] of Camp Margetts); **6,** Changanboerhe (10 miles southwest of Camp Margetts); **7,** Jibuqilehasha.

Moreover, Dashzeveg and Hooker (1997) erected *Irdinolophus* for "*Helaletes* " *mongoliensis* in referring its close relationship with Deperetellidae. Some fragmental specimens of *Colodon*? *grangeri* (Tokunaga, 1933; Takai, 1939) and *C. kushiroensis* (Tomida, 1983) were reported from North Korea and Japan, respectively. In general, previously known helaletids from Asia were represented mainly by maxillae or lower jaws.

Here, we report new material of helaletids, recently unearthed from Huheboerhe area, Erlian Basin, Inner Mongolia, China (fig. 1), which includes a partial cranium with associated left mandible of "*Helaletes*" *fissus* from Duheminboerhe and a partial maxilla of "*Helaletes*" *monogoliensis* from Chaganboerhe. This material provides previously unknown cranial morphologies of Asian early Helaletidae and thus more evidence in understanding their phylogenetic positions. Along with the report of fossils and based on systematic investigations we conducted in the field during the past decade, we also discuss related localities in Huheboerhe area, originally discovered by the Central Asiatic Expedition (CAE) of the American Museum of Natural History.

MATERIALS AND METHODS

Newly described specimens, including skulls and maxillae, are housed in the collections of Institute of Vertebrate Paleontology and Paleoanthropology, Chinese Academy of Sciences, Beijing, China. The terminology of dental structures follows Hooker (1989). For the cranial terminology, we mainly follow Wible (2003) for the general structures and Colbert (2005, 2006) for the proboscis-related structures in tapiroids. The terminology of the petrosal follows O'Leary (2010) and O'Leary et al. (2013, project 773 on MorphoBank [https://morphobank.org/]).

The stack of petrosal photographs was taken using stereoscopic microscope Nikon SMZ-U with camera head Nikon DS-Fi1 and software NIS-Elements F; the photos were then combined into a fully focused image using Helicon Focus 6.3.2 software at the AMNH. Dental measurements were taken using digital calipers to the nearest 0.01 mm.

The phylogenetic analyses were conducted using PAUP 4.0 and TNT 1.1 with a parsimony criterion (Swofford, 2002; Goloboff et al., 2008). The data matrix is composed of 19 taxa and 73 characters (appendixes 1, 2). *Homogalax protapirinus* was selected as an outgroup. The ingroup taxa are listed in appendix 1. Among the ingroup taxa, *Colodon*? *cingulatus* is coded based on the relatively primitive materials (AMNH F:AM 42897–42899) with premolar hypocones not differentitated from protocones, although the holotype of *C.*? *cingulatus*, a maxilla with P3–M1 (CM 722), has more molariform premolars (Radinsky, 1963). As proposed by Radinsky (1963), the difference in the degree of premolar molarization between the two specimens may suggest two distinct species now within *Colodon*? *cingulatus*. The lower teeth of *Paracolodon*? *woodi* were coded based on some materials of *Paracolodon* cf. *P. woodi* (p4–m1, m3) of later Uintan age (Eaton, 1985). Most characters were selected from firsthand observations and comparisons among different species (appendix 1), but some characters were included from previous works. All characters are unordered and equally weighted. The data matrix was deposited in Morphobank (project 2285).

Institutional Abbreviations: **AMNH F:AM,** American Museum of Natural History, Frick Collection, New York; **AMNH FM,** American Museum of Natural History, Fossil Mammals, New York; **CM,** Carnegie Museum of Natural History, Pittsburgh; **IVPP,** Institute of Vertebrate Paleontology and Paleoanthropology, Beijing; **PSS,** Geological Institute of the Mongolian Academy of Sciences, Ulaanbaatar; **USNM,** United States National Museum of Natural History, Smithsonian Institution, Washington, D.C.

SYSTEMATIC PALEONTOLOGY

Class MAMMALIA Linnaeus, 1758
Order PERISSODACTYLA Owen, 1848
Suborder TAPIROMORPHA Haeckel, 1866
Family HELALETIDAE Osborn, 1892
Paracolodon Matthew and Granger, 1925

Type Species: *Paracolodon inceptus* Matthew and Granger, 1925a.
Included Species: *P. fissus*.

Distribution: Middle to late Eocene of Asia.

Diagnosis: Medium-sized helaletid. Canine small and postcanine diastema short. P2–M3 short and wide. P2–4 essentially molariform, hypocone and protocone moderately separated, metaloph usually as prominent as protoloph and extending toward protocone or hypocone, paracone and metacone buccally convex. M1–2 paracone sharp and narrow, metacone short, concave and lingually depressed, centrocrista nearly straight connecting the paracone and the metacone, buccal cingulum adjacent to the metacone prominent. p1 absent. p2–4 with distinct entoconid and deep flexid. m1–3 relatively long and narrow, cristid obliqua highly reduced. m3 hypoconulid highly reduced.

Differential Diagnosis: Differs from *Helaletes* in having P2–4 more molariform, M1–3 metacone more reduced and relatively shorter and wider, p2–4 relatively shorter and wider, more molariform, entoconid more distinct, m1–3 cristid obliqua more reduced, m3 hypoconulid smaller. Differs from *Desmatotherium* in having a smaller canine, P2–3 relatively shorter and wider, P2 more molariform, P2–4 paracone and metacone more convex buccally, M1–3 metacone more concave and slightly more reduced, protoloph and metaloph straight, p3–4 talonid nearly as wide as trigonid. Differs from *Plesiocolopirus* in having P3–4 more molariform, M1–3 metacone concave and more reduced. Differs from *Colodon* (only referred to unequivocal *Colodon occidentalis*) in having a small canine, P1–4 less molariform, paracone and metacone more convex buccally, M1–3 centrocrista nearly straight connecting the paracone and the metacone, m3 hypoconulid smaller, the lateral trough on the ascending process of maxilla extending over the orbit, the medial trough on the dorsal surface of the front separated by a median anterior sagittal crest.

Paracolodon fissus (Matthew and Granger, 1925)

Desmatotherium fissum Matthew and Granger, 1925b: 3, fig. 3.
Helaletes fissus Radinsky, 1965b: 230, fig. 18.
Helaletes fissus Qi, 1987: 39, fig. 28.
Colodon fissus Dashzeveg and Hooker, 1997: 112.

Holotype: AMNH FM 20161: left maxilla with P2–4.

Referred Specimens: AMNH FM 81802: a left mandible with c–m3. AMNH FM 81804: a left mandible with p4–m3.

New Material: IVPP V 22640: an associated cranium and mandible lacking rostral portion; IVPP V 23366.1, a left maxilla with P2–3 and root of P1; and IVPP V 23366.2, an isolated right M3.

Locality and Horizon: Duheminboerhe (Camp Margetts) (IVPP V 22640, V 23366.1), and Daoteyin Obo (IVPP V 23366.2), Erlian Basin, Inner Mongolia; Irdin Manha Formation, middle Eocene.

Diagnosis: Preorbital portion relatively shorter compared with postorbital part. The lateral trough on ascending process of the maxilla extending posteriorly above the supraorbital process of the frontal. A pair of medial troughs on the dorsal surface of the frontal separated by a median anterior sagittal crest and extending posteriorly to the frontal line. P3–4 metaloph

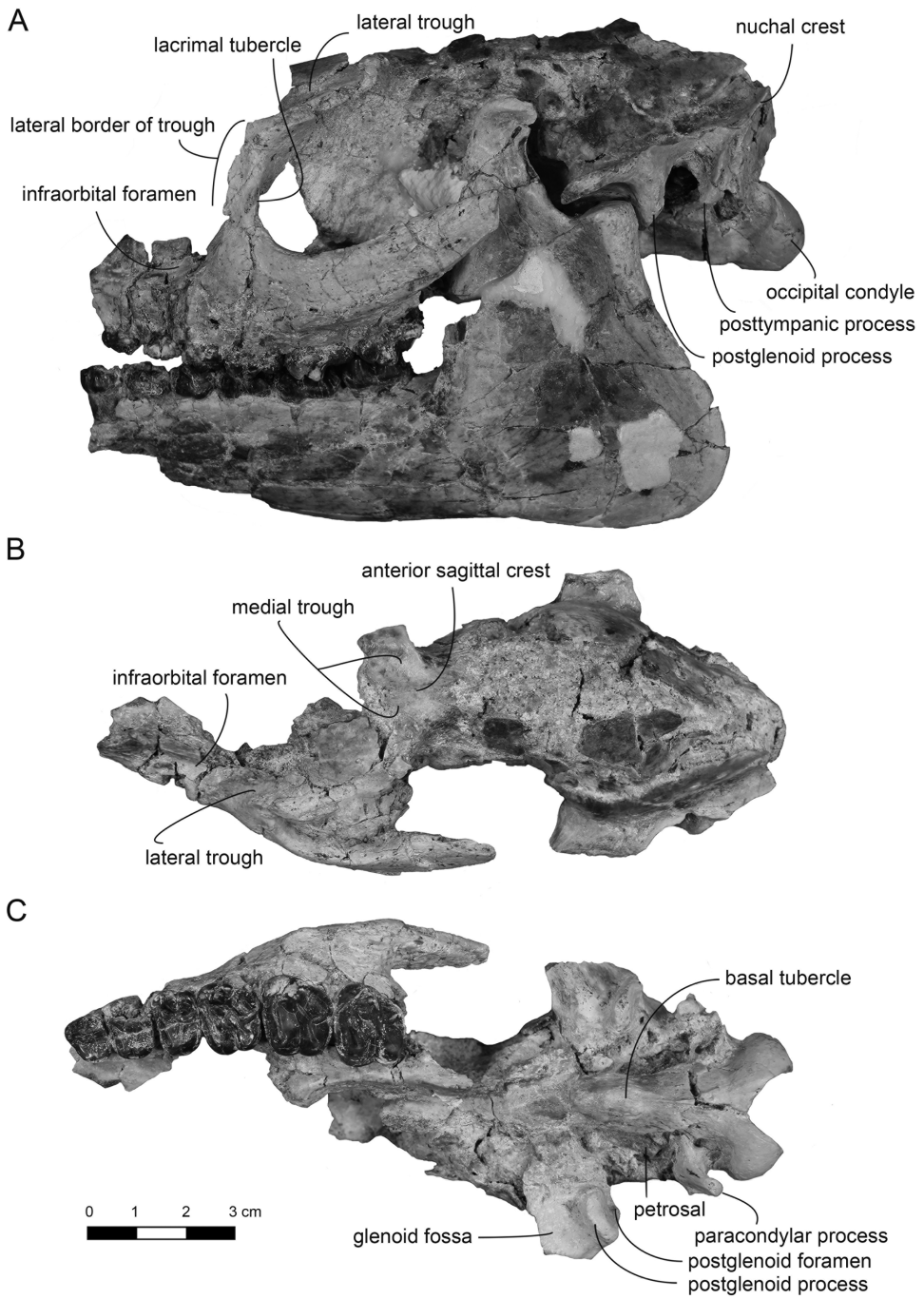

FIG. 2. Cranium and mandible of *Paracolodon fissus* (IVPP V 22640). **A,** lateral view of cranium and mandible; **B–C,** dorsal and ventral views of the cranium.

extending toward protocone, bypassing the hypocone. Posterior end of mandibular symphysis ending at the level of p2. p2–m3 relatively long and narrow. p3–4 entoconid small and distinct, talonid slightly wider than trigonid. m3 hypoconulid highly reduced.

Differential Diagnosis: Differs from *Desmatotherium mongoliense* in having an infraorbital foramen opening above the posterior border of P3, a symphysis of the mandible terminating at the level of p2, P2–4 more molariform, metaloph more prominent and extending toward the protocone, paracone and metacone more convex buccally, M1–2 metacone slightly shorter, M2 paracone vertically situated and more trapezoid in outline, M3 metacone less lingually depressed, p2–4 entoconid smaller, p4 talonid nearly as wide as trigonid, m3 hypoconulid highly reduced. Differs from *Paracolodon inceptus* in being smaller, and in having P3–4 more molariform, P2–4 paracone and metacone more closely situated, M1–2 metacone relatively longer, distobuccal cingulum lower, and M3 metacone less lingually depressed.

Description

Cranium: Of the cranium (IVPP V 22640) only the basicranium and a partial left portion (fig. 2), which was broken off anterior to the orbit, are preserved.

The orbit is rounded and large with the anterior border at the level of the M1 metacone. A small lacrimal tubercle is present on the anterior border of the orbit. Along the anterior border of the orbit there is an incomplete lateral trough presumed for the meatal diverticulum as in *Tapirus*, bordered by a sharp ridge laterally (fig. 2A, B). The lateral trough extends posteriorly over the supraorbital process of the frontal. The infraorbital foramen opens at the level of the anterior border of P4 (fig. 2A, B). The jugal forms the smooth ventral border of the orbit without the postorbital process, and prominently rises backward. A small tubercle is present at the anteroventral border of the jugal above M2. The skull roof is incomplete, although it is clear that a pair of medial troughs are separated by the anterior sagittal crest and extend posteriorly to the frontal lines (fig. 2B); the frontal lines converge posteriorly and likely form a long sagittal crest as in other early perissodactyls. Several nutrient foramina are discernable on the lateral side of the parietal and squamosal. The occipital bone is also fragmentary. The occipital condyles protrude more posteriorly than ventrally, and are widely separated dorsally and closely situated ventrally. The lateroventral border of the condyle (linea divisa condyli) is a somewhat blunt ridge, separating the dorsal and ventral surfaces of the condyles. The preserved ventral part of the nuchal crest on the left side is rather sharp and diverges into two ridges ventrally (fig. 2A): one extending anteriorly above the external acoustic meatus, the other running ventrally along the lateral side of the posttympanic process. Ventrally, the glenoid fossa is flat, and the postglenoid process faces anteriorly and slightly laterally with a postglenoid foramen (fig. 2C). The posttympanic process is short and widely separated from the postglenoid process, while the paracondylar process, preserved on the right side, is stouter and longer than the posttympanic process and curves posteriorly (fig. 2A, C). Medial to the paracondylar process there is a medium-sized hypoglossal foramen (fig. 3). The basioccipital bears a sharp median ridge, which terminates anteriorly at the two parallel basal tubercles (fig. 2C). The basisphenoid extends anterodorsally from the basioccipital.

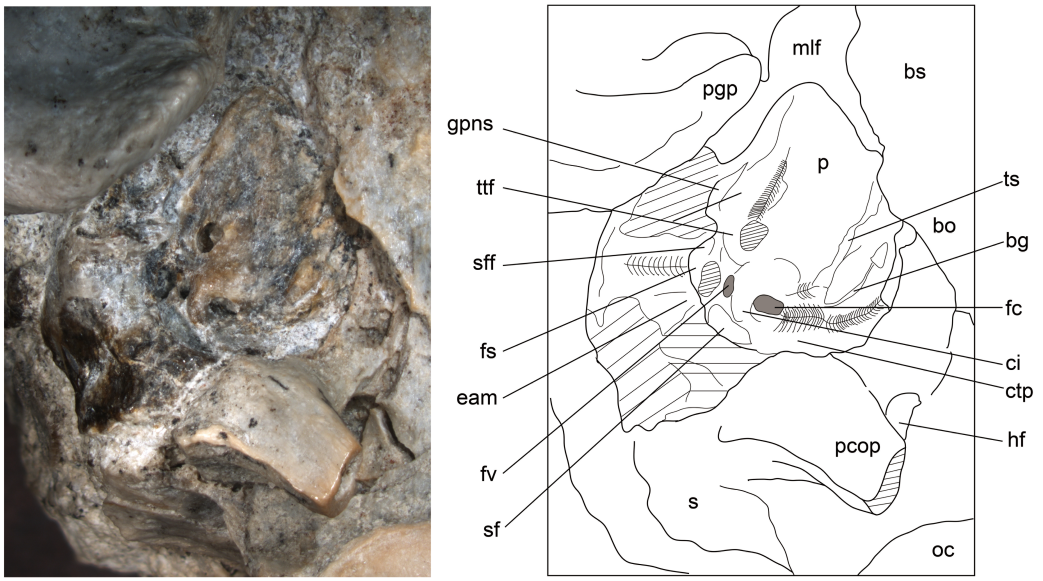

FIG. 3. Right petrosal of *Paracolodon fissus* (IVPP V 22640). Parallel lines indicate damaged surfaces. The anteroposterior length of the promontorium is about 14.66 mm. Abbreviations: **bg,** basicapsular groove; **bo,** basiocciptial; **bs,** basisphenoid; **ci,** crista interfenestralis; **ctp,** caudal tympanic process; **eam,** external acoustic meatus; **fc,** fenestra cochleae; **fs,** facial sulcus; **fv,** fenestra vestibuli; **gpns,** greater petrosal nerve sulcus; **hf,** hypoglossal foramen; **mlf,** middle lacerate foramen; **oc,** occipital condyle; **p,** promontorium; **pgp,** postglenoid process; **pcop,** paracondylar process; **s,** squamosal; **sf,** stapedial muscle fossa; **sff,** secondary facial foramen; **ts,** transpromontorial sulcus; **ttf,** fossa for the tensor tympani muscle.

The right petrosal is preserved in a relatively good condition with its ventrolateral (tympanic) surface exposed on the ventral side (figs. 2C, 3). The promontorium is almond shaped and pointed anteriorly; however, the bone is damaged at the posterolateral margin (indicated by cross-hatching in fig. 3). The surface of the promontorium is uneven with the lateral portion situated more toward the cerebellar surface and the medial part relatively flat. A depression in the shape of a groove runs along the posterolateral side. We interpret this depression as the fossa for the tensor tympani muscle. Lateral to this fossa is a narrow and short groove, which is separated from the former by a distinct ridge. This groove may have been for the greater petrosal nerve, the anterior branch of the facial nerve. An unambiguous hiatus Fallopii is not discernable on the specimen either because the hiatus was absent or not preserved. Thus, whether the greater petrosal nerve branched within the petrosal bone and then passed through a hiatus Fallopii or the hiatus Fallopii was absent and the greater petrosal nerve branched within the middle ear and extended forward cannot be determined. On the medial side of the promontorium, there is another groove that extends from the anteromedial side of the fenestra cochleae (fenestra rotundum), and parallels the lateral border of the promontory. This groove has a pronounced lateral ridge. We tentatively interpret this groove as the transpromontorial sulcus, and it may have been made by the internal carotid artery, internal carotid plexus, tympanic plexus, or all of these structures. We note, however, that it is also possible that a pronounced lateral ridge of the transpromontorial sulcus was the attachment site for a tympanic bulla that is not preserved. Such an

arrangement of the bulla might have meant that the internal carotid artery would have been external to the tympanic bulla (extrabullar). A short and narrow groove present medial to the transpromontorial sulcus may be the basicapsular groove for the inferior petrosal sinus. Between these two grooves the surface is swollen and has a pronounced bump.

The fenestra cochleae is situated on the posterolateral corner of the promontorium, rounded, and facing posteriorly. On the anterolateral side of the fenestra cochleae and considerably smaller than the fenestra cochleae is an oval-shaped fenestra vestibuli (fenestra ovalis) that faces ventrolaterally, indicating a relatively small base of the stapes. The crista interfenestralis is relatively protruded, somewhat swollen between the two fenestrae, becoming laterally compressed posteriorly, and terminating at the anterior margin of the stapedial muscle fossa. The caudal tympanic process is mediolaterally broad. A jugular foramen, which would have been located on the posteromedial side of the caudal tympanic process, is filled by matrix. The fossa for the stapedial muscle is relatively large and roughly triangular, situated on the posterolateral side of the fenestra cochleae and posterior side of the fenestra vestibuli. Anterior to the stapedial muscle fossa is a facial sulcus, which is partially broken off on the right side but more complete on the left side. The facial sulcus emerges anteriorly from a relatively large secondary facial foramen, which is situated anterolaterally relative to the fenestra vestibuli. Lateral to the facial sulcus is an incomplete external acoustic meatus, widening laterally. The epitympanic recess, which would have housed the articulation of the malleus and incus in life, is not preserved. The tegmen tympani is broken and not complete, however, its dorsolateral surface appears to have been convex as deduced from the preserved part.

Mandible: The horizontal ramus of mandible anterior to p2 was broken off, and the ventral border below the premolars was broken (fig. 2A). The preserved horizontal ramus is relatively slender with a slightly convex ventral border. The vessel notch is wide and shallow. The angle is rounded with thin margins, extending posteriorly beyond the condyle. The condyle is relatively high, and the distance between the condyle and the alveolar border is roughly equal to the length of m1–3. The condyle has a tear-shaped and nearly flat articular surface for the glenoid fossa with an apex toward the medial and slightly ventral side. The facet curves onto the posterior surface of the condyle on the medial end. The lateral side of the posterior surface of the condyle is rugose. The coronoid process is higher than the condyle with a truncated dorsal rim, and nearly vertically placed. The mandibular notch is generally concave with a slight convexity in the middle. The anterior border of ascending ramus is straight and slightly posteriorly slanted from the lateral view. The ventral half of the anterior border of the ascending ramus is a deeply concave fossa. On the lateral surface of the ascending ramus there is a relatively deep masseteric fossa.

Upper Teeth: P1: A broken alveolar and an appressed surface anterior to the parastyle of P2 indicate the presence of P1 (figs. 2C, 4A).

P2: The tooth is roughly quadrilateral in outline with the width considerably greater than the length (fig. 4A). The paracone and metacone are nearly equal in size and closely situated with convex buccal surfaces. The parastyle is smaller and slightly lower than the paracone, situated mesial to the latter. The metastyle is relatively distinct, but much smaller than the paras-

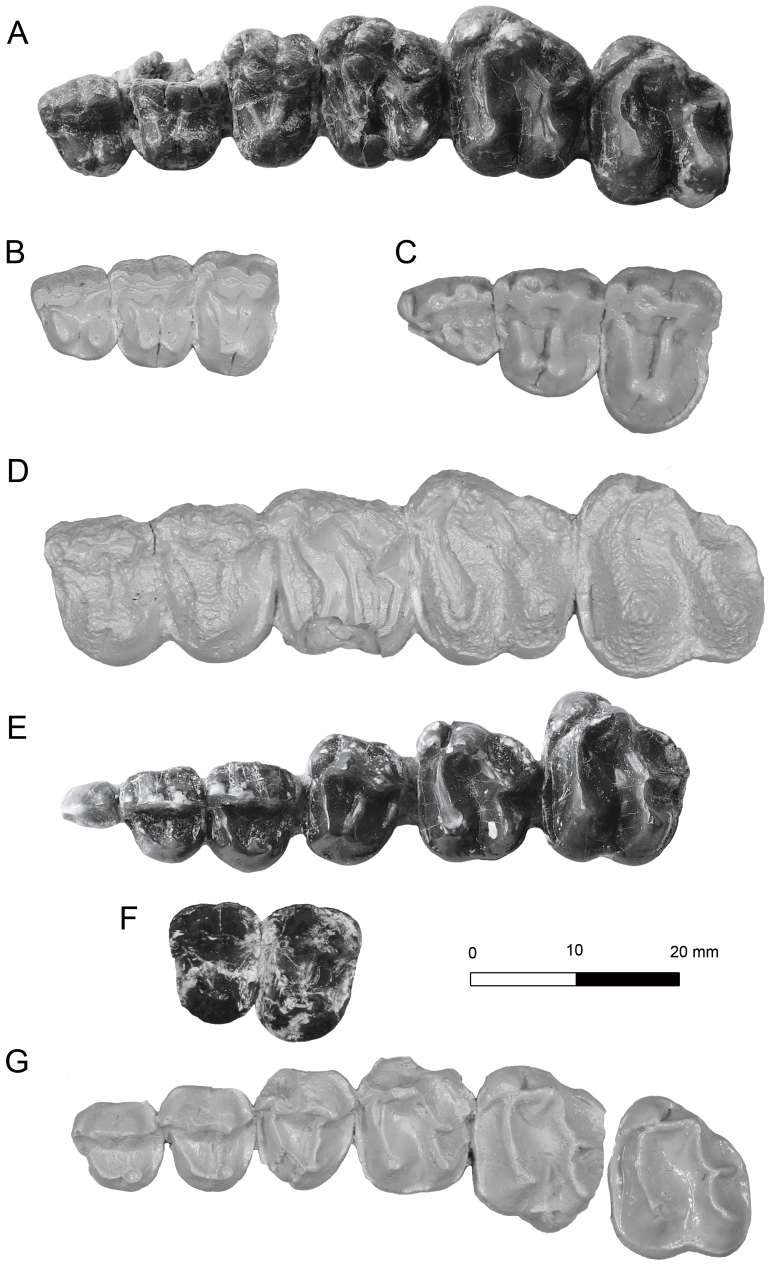

FIG. 4. Occlusal view of upper cheek teeth of *Paracolodon fissus*, *Paracolodon inceptus*, and *Desmatotherium mongoliense*. **A–B,** *P. fissus*; **A,** left P2–M3 (IVPP V 22640); **B,** left P2–P4 (AMNH FM 20161); **C–D,** *P. inceptus*; **C,** left P1–P3 (AMNH FM 20355); **D,** left P3–M3 (AMNH FM 20357); **E–G,** *D. mongoliense*; **E,** left P1–M2 (IVPP V 14692); **F,** left P3–P4 (AMNH FM 20156); **G,** left P2–M3 (AMNH FM 19161, reversed).

tyle. The protoloph extends from the protocone toward the joint of the parastyle and the paracone, and stops before its contact with the ectoloph. The hypocone is separated from the protocone by a deep furrow on the lingual side, and is slightly more lingually situated than the protocone. The metaloph is indistinct. The weak mesial and distal cingula are present.

P3–4: The ectoloph of P3 was broken off. The morphology of P3 is similar to that of P2 (fig. 4A). However, the hypocone of P3 is as lingually situated as the protocone, and the metaloph is distinct extending from the mesiolingual slope of the metacone to the protocone, bypassing the hypocone. The P4 is similar to P3, but the former is much wider and relatively shorter than P2 and P3. The paracone and metacone are conical and closely placed, with the metacone slightly smaller and more lingually situated than the paracone. The parastyle is relatively small and slightly buccal to the paracone. The hypocone is separated from the protocone by a shallow furrow on the lingual side.

M1–2: These teeth are similar in morphology, except M2 is larger (fig. 4A). The parastyle of M1–2 is large, slightly buccally situated to the paracone, and compressed to the protoloph. The paracone is conical, relatively high and sharp, and vertically placed. A broadly convex crest is present on the lingual side of the paracone. The metacone is strongly lingually depressed with a concave buccal surface and a rather reduced postmetacrista. The position of the metacone is nearly midway between the paracone and the hypocone. The protocone and the hypocone are equal in size. The protoloph extends from the protocone to the parastyle, joining the preparacrista buccally, which is mesiodistally extended. The metaloph is much shorter than the protoloph, joining the ectoloph at the apex of the metacone. The buccal cingulum adjacent to the metacone is well developed and almost forms a small platform. The mesial and distal cingula are also distinct, while the lingual cingulum is absent. The buccal base of the paracone also lacks the cingulum.

M3: The tooth is roughly similar to M1–2 (fig. 4A), however, M3 differs from M1–2 in having an apex of paracone distally curved, a metacone less lingually depressed and more reduced, and a centrocrista relatively shorter than the metaloph and aligned with the metaloph. Furthermore, the platformlike buccal cingulum adjacent to the metacone on M3 extends to the distal border, and a prominent cingulum is present at the lingual base of the central valley.

Lower Teeth: p2: The tooth bears a conical protoconid in the middle, from which a short paracristid extends anteriorly to a high paraconid (fig. 5A). The paraconid is separated from the protoconid by a deep groove on the lingual side. The metaconid is absent. The hypoconid is large, nearly as high as the paraconid, and situated in the middle of the posterior border. The cristid obliqua is slightly lingually concave. A small, rudimentary entoconid is appressed to the lingual side of the hypoconid. The cingulum is absent.

p3: The crown of the tooth is partially broken. The tooth is rectangular in outline (fig. 5A). It can be deduced from the preserved portion that the paraconid is relatively high, the metaconid is smaller than the protoconid, the hypoconid is prominent, and the entoconid is small but distinct.

p4: The crown of the tooth is rectangular in outline (fig. 5A). The trigonid is wider than long, and slightly shorter and narrower than the talonid. The protoconid and the metaconid are conical, equal in size with the latter more distally situated than the former. The protolophid

FIG. 5. Occlusal view of lower cheek teeth of *Paracolodon fissus* and *Desmatotherium mongoliense*. **A–B,** *P. fissus*; **A,** left p2–m3 (IVPP V 22640); **B,** left p2–m3 (AMNH FM 81802); **C–D,** *D. mongoliense*; **C,** left p3–p4 (AMNH FM 81718, reversed); **D,** left p3–m3 (AMNH FM 20155, reversed).

is moderately notched in the middle. The paracristid extends from the protoconid mesially and slightly lingually, and then curves lingually along the mesial border. The hypoconid is conical, large, and lower than the protoconid, extending the cristid obliqua to the distolingual side of the protoconid. The entoconid is small but as distinct as in p3. The hypolophid and the cingulum are absent.

m1–2: The m1 is similar to m2 in morphology, but m2 is slightly larger than m1 (fig. 5A). The trigonid of m1–2 is similar to that of p4, except that the metaconid is more separated from the protoconid and the protolophid is nearly transversely extended and slightly notched. The talonid is slightly narrower and considerably longer than the trigonid, and the hypolophid is more oblique than the protolophid. The cristid obliqua is rather reduced. A weak ridge anterobuccally extends from the entoconid. A small hypoconulid is present. An anterobuccal cingulum is present.

m3: The tooth is similar to m1 and m2 except for a more distinct hypoconulid (fig. 5A).

Comparisons and Discussion

Skull and Teeth: Osborn (1923) erected *Desmatotherium mongoliense* based on materials from Irdin Manha Formation, Irdin Manha escarpment. Some of the specimens included in the species were later recognized as belonging to *Lophialetes* (Matthew and Granger, 1925a). The main diagnostic feature for *D. mongoliense,* according to Osborn (1923), is that P2–3 has a "duplicate internal cusp" similar to *Desmatotherium intermedius* (= *D. guyotii*). Similarly, Matthew and Granger (1925a) figured and discussed *Desmatotherium mongoliense* in more detail, and named another species *Desmatotherium fissum*.

Matthew and Granger (1925b) erected *Colodon inceptus* and *Paracolodon curtus* based on specimens from Ergilin Dzo (Ardyn Obo), Mongolia. They distinguished *Colodon inceptus* from *C. occidentalis* on the grounds that the former has a nearly straight centrocrista on molars connecting the paracone and the metacone, in contrast to the centrocrista that curves buccally just behind the paracone in *C. occidentalis*. Matthew and Granger (1925b) distinguished *Paracolodon* from *Colodon* mainly based on the absence of P1, short postcanine diastema, and molar relatively larger as inferred from the partial alveolus.

Radinsky (1963) regarded *Desmatotherium* as a junior synonym of *Helaletes*, and later he (Radinsky, 1965a) assigned both *D. mongoliense* and *D. fissum* to *Helaletes* based on the degree of premolar molarization and relatively long and narrow proportions of M1, P2–4, and p2–3 (for "*H.*" *mongoliensis*), or P2–4 metalophs less prominent than the protolophs and extending toward the protocones (for "*H.*" *fissus*). However, some authors still considered *Desmatotherium* a valid genus (Schoch, 1989; Colbert and Schoch, 1998). Radinsky (1965a) also considered that specimens on which *Colodon inceptus* and *Paracolodon curtus* were respectively based actually represent a single species; he combined them into *Colodon inceptus*.

Since the revision of Asian Paleogene tapiroids by Radinsky (1965a), Dashzeveg and Hooker (1997) have continued to work on *Helaletes* and *Colodon* and assigned the specimens of "*Helaletes*" *fissus* to *Colodon* and suggested its close relationship with *C. inceptus*; they erected *Irdinolophus* for "*Helaletes*" *mongoliensis*, suggesting its close relationship with Deperetellidae (discussed below).

The new material reported here is nearly identical to the holotype of "*Helaletes*" *fissus* (AMNH FM 20161), represented by a left maxilla with P2–4 (fig. 4B; table 1). However, AMNH FM 20161 has a more separated and larger hypocone compared with the protocone on P2 and relatively weaker metalophs on P3–4. In our view, these subtle differences are due to individual variation of the species. The mandible of "*H.*" *fissus*? (AMNH FM 81802) is very similar to that of IVPP V 22640 (fig. 5A, B), except that the former is slightly smaller (table 2) and has a smaller and lower paraconid on p2–3, an incipient metaconid and a more basined talonid on p2, and a slightly more reduced paralophid on m2–3. We attribute these differences to individual variation, and assign the specimen (AMNH FM 81802) to "*H.*" *fissus*.

Dashzeveg and Hooker (1997) recognized some similarities between "*Helaletes*" *fissus* and "*Colodon*" *inceptus* in that both shared premolars with incipient molarization and were lacking lingual cingula, with lower molars relatively narrow, and m3 hypoconulid reduced to a cingular bulge. We agree with Dashzeveg and Hooker (1997) that "*Helaletes*" *fissus* and

TABLE 1. Measurements of upper cheek teeth of *Paracolodon fissus*, *Paracolodon inceptus*, and *Desmatotherium mongoliense* (mm).

	P. fissus		*P. inceptus*		*D. mongoliense*		
	IVPP V 22640	AMNH FM 20161	AMNH FM 20355	AMNH FM 20357	IVPP V 14692	AMNH FM 19161	AMNH FM 20156
P1 L			9.60		6.30		
P1 W			9.30		4.57		
P2 L	7.92	7.38	11.09		8.21	8.44	
P2 W	9.90	9.62	13.13		9.31	9.42	
P3 L	9.18[a]	8.56	11.76	11.29	8.73	8.89	8.72
P3 W	11.05[a]	11.24	16.45	15.28	11.11	11.43	12.19
P4 L	9.27	8.80		11.17	9.24	10.09[a]	9.71
P4 W	13.34	12.36		16.57	12.63	12.98	13.65
M1 L	11.65			14.56	11.62	11.45[a]	
M1 W	14.86			17.08[a]	13.67	14.14[a]	
M2 L	13.92			16.47	13.90	14.52	14.20
M2 W	16.38			19.13	16.30	15.16	15.47
M3 L	14.30			17.00		14.35	
M3 W	16.20			20.37		15.67	
P2–4 L	27.41[a]	24.71			26.57	27.41	
M1–3 L	41.05			49.11		40.17	

[a] Approximate.

"*Colodon*" *inceptus* are closely related, and consider that they share several other features, including M1–2 centrocrista less aligned with the metaloph, the upper molar centrocrista straight, the metacone considerably lingually depressed and short with a prominent buccal cingulum, and P2–4 paracone and metacone convex buccally, the protoloph extending toward the parastyle and fading out before reaching to the ectoloph (fig. 4A–D; table 1). We note that P3–4 of "*Helaletes*" *fissus* is more molariform than that of "*Colodon*" *inceptus* in having the protocone and hypocone more separated by a distinct lingual groove, whereas P2 of "*Colodon*" *inceptus* is more molariform than that of "*Helaletes*" *fissus* in having a quadrate outline in occlusal view and a stronger metaloph.

It is uncertain whether "*Helaletes*" *fissus* and "*Colodon*" *inceptus* should be included in the genus *Colodon*. Radinsky (1965a: 232) thought that "*Colodon*" *inceptus* is different from *Colodon occidentalis* in having a small upper canine, a relatively longer P1 with separated paracone and metacone, more convex P2–4 paracone not so merged into the ectoloph, P3–4 hypocone not so well differentiated from the protocone, and M2–3 paracone narrower and less extended distally. These differences also distinguished "*Helaletes*" *fissus* from *Colodon occidentalis*, except that C1 and P1 were unknown in "*Helaletes*" *fissus*. The lower cheek teeth of "*Helaletes*" *fissus* further differ from those of *Colodon occidentalis* in being relatively longer and narrower, and in having a small c1, premolars much less molariform with smaller entoconids and talonids slightly wider than the trigonids, and m3 with much smaller hypoconulid.

TABLE 2. Measurements of lower cheek teeth of *Paracolodon fissus* and *Desmatotherium mongoliense* (mm).

	P. fissus		*D. mongoliense*	
	IVPP V 22640	AMNH FM 81802	AMNH FM 81718/20155	AMNH FM 81803
p2 L	8.33	7.54		8.13
p2 W	6.23	5.29		5.61
p3 L	9.70[a]	8.32	9.62/	9.30
p3 W	7.47[a]	6.55	7.21/	6.81
p4 L	9.39	8.59	9.81/9.85	9.24
p4 W	7.84	7.64	8.60/8.78	7.93
m1 L	11.81	11.63	/11.94	12.43
m1 W	8.58	8.30	/9.20[a]	8.80
m2 L	13.09	13.12	/13.51	14.08
m2 W	9.74	9.24	/10.57	9.53
m3 L	15.11	14.50	/17.2a	
m3 W	10.16	9.57	/9.9	
p2–4 L	28.2	24.82		27.7
m1–3 L	40.51	39.39		

[a] Approximate.

The skull of "*Helaletes*" *fissus* (IVPP V 22640) further differs from that of *Colodon* described by Colbert (2005) in having the following characters (fig. 2A–C): the lateral trough on the ascending process of the maxilla extending posteriorly over the supraorbital process of the frontal rather than terminating in a fossa, the frontal with a pair of anteroposteriorly extended medial troughs separated by a median anterior sagittal crest rather than dorsally inflated, the anterior border of the orbit above the boundary of M1 and M2 rather than above M1, and a relatively small lacrimal tubercle. Although the rostral part of the skull in IVPP V 22640 is not preserved, another mandibular specimen (AMNH FM 81802) with the symphysis has a relatively short symphysis and postcanine diastema, suggesting a relatively shorter preorbital skull length of "*Helaletes*" *fissus* to that of *Colodon*. "*Colodon*" *inceptus* also has a rather short postcanine diastema, indicating a similar short preorbital skull length as in "*Helaletes*" *fissus*.

In conclusion, both dental and especially cranial characters indicate that "*Helaletes*" *fissus* and "*Colodon*" *inceptus* belong to the same genus that differs from *Colodon*. Thus, we resumed the genus *Paracolodon* for these two species: *P. fissus* and *P. inceptus*. The possibility that the middle Eocene Irdinmanhan *P. fissus* is generically distinct from the later Eocene Ergilian *P. inceptus* cannot be ruled out, pending discovery of more complete material of *P. inceptus*.

Although the genus *Desmatotherium* was synonymized with *Helaletes* by Radinsky (1963), some authors still regarded *Desmatotherium* as a valid genus based on its larger size, the metalophs bypassing the hypocones on P3–4, and highly reduced hypoconulid on m3 (Schoch, 1989; Colbert and Schoch, 1998). *Paracolodon fissus* is similar to *Desmatotherium intermedius* in having the P3–4 metaloph extending toward the protocone, bypassing the hypocone. However, *P. fissus* is mainly distinguished from *D. intermedius* by teeth relatively shorter and wider

(figs. 6–8), P2 more molariform with distinct hypocone, P2–4 paracone and metacone more convex and more closely situated, P3–4 protoloph extending toward the parastyle and fading out before its contact with the ectoloph, P4 metacone slightly more lingually depressed, upper molar metacone more lingually depressed, more concave, and shorter, protoloph and metaloph straight and less mesially convex, and p3–4 talonid nearly as wide as the trigonid.

In terms of size and morphology, the upper molars of *P. fissus* are rather similar to those of "*Colodon*" *kayi* and "*Colodon*" *woodi*, both of which were originally assigned to *Desmatotherium* by Hough (1955) and Gazin (1956). Radinsky (1963) referred "*Desmatotherium*" *kayi* and "*Desmatotherium*" *woodi* to *Colodon* mainly based on their molariform P3–4, and this assignment was followed by following authors (Eaton, 1985; Tabrum, 2012). On the other hand, upper molars of "*Colodon*" *kayi* and "*Colodon*" *woodi* are similar to those of *Paracolodon fissus*, but different from those of *Colodon occidentalis*, in having approximately equal size, straight centrocrista, the paracone relatively higher and sharper, and M2 metacone slightly less reduced (Matthew and Granger, 1925b; Hough, 1955; Radinsky, 1963). The upper premolars of "*Colodon*" *kayi* and "*Colodon*" *woodi* are further similar to those of *P. fissus* in having more buccally convex paracone and metacone and less separated protoloph and metaloph compared with those of *Colodon occidentalis*. The lower premolars of "*Colodon*" *kayi* are somewhat intermediate between *P. fissus* and *C. occidentalis* in proportion and morphology. However, the presence of the lower canine, the deep buccal fold on p2–4 (Radinsky, 1963), and the m3 hypoconulid strongly reduced are features that are more similar to those of *P. fissus*. However, *P. fissus* is mainly different from "*C.*" *kayi* and "*C.*" *woodi* in having less molariform upper premolars with metaloph extending toward the protocone, upper molars with more lingually depressed metacone, and lower premolars relatively longer and narrower with smaller entoconid. As a result, we are skeptical of the referral of *kayi* and *woodi* to *Colodon*, and we suggest assigning the species in *Colodon*? *kayi* and *Colodon*? *woodi*.

Petrosal: Because the new specimen (IVPP V 22640) preserves the relatively complete petrosal, it gives us an opportunity to investigate the morphology of petrosals of early perissodactyls. There are not many previous studies on early perissocdactyl petrosals. Paleogene perissodactyl petrosals that were mentioned or described with or without illustrations include *Hyracotherium*, *Orohippus* (Cifelli, 1982), *Pachynolophus* (Savage et al., 1965), *Heptodon* (Radinsky, 1965b; Cifelli, 1982), *Schlosseria* (Li and Wang, 2010), *Hesperaletes* (Colbert, 2006), *Litolophus* (Bai et al., 2010), and cf. *Protitanotherium* (Mader, 2009). Furthermore, petrosals of extant *Equus* and *Tapirus* have also been described (Sisson et al., 1975; O'Leary, 2010). Detailed comparisons and studies of perissodactyl petrosals are beyond the scope of present paper, so we focus our discussion on certain characters related to our new specimens.

The petrosal of *Paracolodon fissus* is characterized by the relatively medially situated transpromontorial sulcus, while in other known perissodactyls the transpromontorial sulcus is either absent or more laterally situated. The promontorium of perissodactyls were usually considered to be smooth, without traces of grooves for the internal carotid artery/plexus or stapedial artery (Wible, 1986). The internal carotid artery is medial to the auditory bulla and middle ear cavity (extrabullar) (Wible, 1986). However, Li and Wang (2010) described the petrosal of *Schlosseria* with three grooves on the promontorium, the sulcus for medial ramus of internal

carotid artery, the stapedial artery sulcus, and promontory artery sulcus. We suspect that "the sulcus for medial ramus of internal carotid artery" in *Schlosseria* needs to be further investigated, because eutherians usually have a single internal carotid artery in the lateral groove, and the medial groove was usually for the inferior petrosal sinus (Wible, 1983; 1986). Colbert (2006) mentioned that the petrosal of *Hesperaletes* has a distinct transpromontory sulcus, running anteriorly from the fenestra cochleae. In *Paracolodon fissus*, we suggested that a medial groove probably represents the transpromontorial sulcus for the following reasons: First, the groove is too ventrally displaced to be the basicapsular groove, which is for the inferior petrosal sinus. In *Tapirus* and *Equus*, as well as many artiodactyls, the basicapsular groove is on the dorsal surface (O'Leary, 2010). On the other hand, the basicapsular grooves in a few groups (such as hippopotamids) with ventrally placed positions run along the medial border (O'Leary, 2010). Furthermore, we considered that a more medially situated, narrower groove probably represents the basicapsular groove. Second, the groove is relatively wide, which was likely not made by a single soft tissue, but may have been made by internal carotid artery, internal carotid plexus, and/or tympanic plexus corresponding with the transpromontorial sulcus.

The promontorium of *Paracolodon* is almond shaped, which is similar to that of *Schlosseria* and *Hesperaletes*, but different from hemiellipsoid promontorium in *Heptodon* and *Tapirus*. The petrosal of *Paracolodon* is similar to those of *Heptodon* and *Tapirus* in having the fenestra cochleae considerably larger than the fenestra vestibuli. The hiatus Fallopii is ventrally situated in *Hyracotherium*, *Orohippus*, and *Heptodon*, whereas that of *Tapirus* is situated anterior to the tegmen tympani. Unfortunately, the hiatus Fallopii in *Paracolodon* was uncertain, either absent or not preserved. The dorsolateral tegmen tympani of *Paracolodon fissus* is prominently convex, whereas that of *Tapirus* is flat.

Genus *Desmatotherium* Scott, 1883

Type Species: *Desmatotherium intermedius* (Osborn, Scott and Speir, 1878).

Included Species: *D. mongoliense.*

Distribution: Middle Eocene of Asia and North America.

Diagnosis: Medium-sized helaletid. Canine relatively large and postcanine diastema long. P2–M3 relatively long and narrow. P2–4 submolariform, hypocone and protocone separated to varying extent, metaloph extending toward hypocone or protocone. M1–3 metacone relatively short and lingually depressed, protoloph and metaloph slightly convex mesially, buccodistal cingulum prominent. M1 metacone very slightly convex, M2 paracone distally curved at the apex. p1 absent. p2–4 entoconid distinct and buccal cingulum prominent, p3–4 talonid wider than trigonid. m1–3 cristid obliqua highly reduced.

Differential Diagnosis: Differs from *Helaletes* in having P2–4 more molariform, M1–3 metacone shorter and more lingually depressed, p2–3 more molariform with more prominent entoconid, m1–3 cristid obliqua more reduced, m3 hypoconulid much weaker. Differs from *Paracolodon* in having longer postcanine diastema, upper cheek teeth relatively longer and narrower, P2 less molariform, M1–3 metacone slightly less reduced. Differs from *Colodon* in

having premolars less molariform, M1–3 centrocrista extending straight from paracone to metacone, metacone less reduced, m1–3 paralophid less reduced. Differs from *Hesperaletes* in having a postcanine diastema relatively shorter, P2–4 more molariform, M1–3 parastyle more closely appressed to paracone, metacone slightly less convex, more reduced and more lingually situated, metaloph joining the apex of the metacone, p2–4 more molariform, m1–3 cristid obliqua more reduced, and in lacking p1. Differs from *Plesiocolopirus* in having P2–M2 relatively longer and narrower, P2–4 hypocone and protocone more separated, paracone and metacone slightly less convex, M1–2 metacone less reduced and only slightly convex.

Desmatotherium mongoliense (Osborn, 1923)

Desmatotherium mongoliense Osborn, 1923: 2.
Desmatotherium mongoliense Matthew and Granger, 1925b: 1, figs. 1–2.
Helaletes mongoliensis Radinsky, 1965a: 227, figs. 16–17, pl. 4: figs. 1–4.
Helaletes mongoliensis Reshetov, 1979: 15, pl. 1: fig. 4.
Irdinolophus mongoliensis Dashzeveg and Hooker, 1997: 113, figs. 4, 10.

Holotype: AMNH FM 19161: Right maxilla with P2–M3.

Referred Specimens: AMNH FM 20155: right mandible with p3–m3; AMNH FM 20156: left maxilla with P3–4, right maxilla with M2; AMNH FM 81717: right mandible with p3–m1; AMNH FM 81718: right mandible with p3–4; AMNH FM 81792: right mandible with dp4–m1; AMNH FM 81803: right mandible with p2–m2; PSS.41–3: right M1/2.

New Material: IVPP V 14692: left maxilla with DP1, P2–M2; IVPP V 23367, associated upper cheek teeth with right P2–3, left P2–3, M1/2, and M3; IVPP V 23368, a right mandible with p2–4; IVPP V 23369.1, a right P3; IVPP V 23369.2, a left P4; IVPP V 23369.3, a right M3; IVPP V 23369.4, a right m3 talonid; IVPP V 23369.5–6, two left m3.

Locality and Horizon: Irdin Manha escarpment (IVPP V 23368, V 23369.1–2, 4), Duheminboerhe (IVPP V 23367), Huheboerhe (IVPP V 23369.3, 5), and Chaganboerhe (IVPP V 14692, V 23369.6), Erlian Basin, Inner Mongolia; Irdin Manha Formation, middle Eocene. Mergen, eastern Gobi, Mongolia; Mergen Formation, middle Eocene.

Diagnosis: The ascending process of maxilla with a wide and shallow lateral trough. Infraorbital foramen opening above the posterior end of P4 indicating a short infraorbital canal. Symphysis terminating anterior to p2. P2–4 relatively long and narrow, protocone distally extended with the hypocone rudimentary separated. P2–3 metaloph greatly reduced compared with protoloph. M1–2 metacone concave, short, lingually depressed. The apex of M2 paracone distally curved. M3 metacone highly reduced. p2–4 entoconid large, p4 talonid wider than trigonid. m3 with a rather small hypoconulid.

Differential Diagnosis: Differs from *Desmatotherium intermedius* in having P2 hypocone and protocone slightly more separated, P3–4 metaloph extending toward hypocone instead of protocone, M1–3 metacone more lingually depressed, M2–3 centrocrista more aligned with metaloph, M3 more trapezoid in outline, p3–4 talonid not considerably wider than trigonid, and m3 hypoconulid more distinct.

Description

DP1 (P1): The tooth is anteriorly slanted as compressed by P2 (fig. 4E). The color of the enamel is light brown, lighter than black-brown enamels of other teeth, suggesting a deciduous tooth. DP1 is roughly oval in occlusal outline with two roots. A main cusp is present in the middle of the crown, extending a short ridge mesially to the indistinct parastyle, and then slightly curving lingually. A ridge extends distally from the main cusp terminating in a more distinct and slightly higher cusp compared with the parastyle. This distal cusp probably represents the rudimentary metacone. The buccal side of the ectoloph is slightly convex. A ridge extends from the lingual base of the main cusp distolingually, and another ridge extends from the apex of the metacone lingually along the distal border. Two ridges are separated by a shallow notch on the lingual side. A cingulum is absent.

P2: The tooth is roughly rectangular in outline and relatively long and narrow (fig. 4E). The paracone and metacone are equal in height and closely situated. Both of them are slightly convex on the buccal surface and merged with the ectoloph. The parastyle is distinct and mesial to the paracone, whereas the metastyle is indistinct and lower. The strong protoloph extends toward the parastyle, fading out before its contact with the ectoloph. A ridge extends from the protocone distally and even beyond the hypocone. The protocone and the hypocone are separated by a faint groove on the lingual side. A tiny cuspule is present in the valley between the hypocone and the metacone, representing the metaconule. A weak ridge connects the hypocone and the metaconule. The mesial cingulum is weak, whereas the distal cingulum is considerably stronger. The buccal cingulum is weak and somewhat interrupted at the paracone, and the lingual cingulum is absent.

P3: The P3 is similar to P2, but is relatively shorter and wider (fig. 4E). It further differs from P2 in having the protoloph in contact with the parastyle, the hypocone slightly more lingually situated compared with the protocone, and the metaloph completely absent.

P4: The P4 is relatively shorter and wider than P2–3 (fig. 4E). The paracone and metacone are equal in height, but more separated from each other than those of P2–3. The metacone is less convex and slightly more lingually situated than the paracone. The parastyle is more readily discriminated from the ectoloph than that of P2–3. The protoloph extends toward the junction of the parastyle and the preparacrista. The protocone and the hypocone are separated by a relatively distinct groove on the lingual side. The metaloph is as strong as the protoloph, extending from the hypocone to the mesiolingual base of the metacone, but separated from the latter by a shallow valley.

M1: The tooth is moderately worn and roughly square in outline (fig. 4E). The paracone is broadly convex, while the metacone is strongly lingually depressed and rather short with a slightly convex buccal surface. The postmetacrista is distobuccally extended. The parastyle is large, situated mesially to the paracone and closely appressed to the latter. The protoloph extends toward the preparacrista. The metaloph is about half of the protoloph length, joining the ectoloph at the apex of the metacone. A faint crest is present on the lingual surface of the paracone and nearly vertically placed. A weak cingulum is present on the mesial side, distal side, and the lingual opening of the middle valley. A prominent buccal cingulum is present adjacent to the metacone, although this portion is partially broken.

M2: The M2 is similar to M1 in morphology, but M2 is considerably larger than M1 (fig. 4E). M2 is further different from M1 in that the buccal side of the tooth is longer than the lingual side, the apex of the paracone curves distally as deduced from the direction of the lingual crest, and the parastyle is relatively and absolutely larger.

Comparisons and Discussion

The new material is very similar to the holotype of "*Helaletes*" *mongoliensis* (figs. 4G, 6; table 1), especially in their degree of premolar molarization, in which P2–3 protocone is distally extended, the hypocone is rudimentarily separated from the protocone, and the metaloph is much reduced as compared with the protoloph (fig. 4E, G). They are further similar in having premolars relatively long and narrow, paracone and metacone merged with the ectoloph, M1–2 paracone broadly convex with the apex of the paracone nearly vertically situated on M1, and distally inclined on M2, metacone strongly lingually depressed and short, and infraorbital foramen opening above the posterior border of P4. However, the new material is different from the holotype in having P2 protocone and hypocone less separated on the lingual side, and P3 lacking the metaloph—all due to individual variation.

The type of "*Helaletes*" *mongoliensis* (AMNH FM 19161), the right maxilla with P2–M3, was collected from Irdin Manha Formation at Irdin Manha escarpment, 23 miles south of Iren Dabasu in 1922. All other referred specimens housed at the AMNH were collected from Irdin Manha Formation at Irdin Manha escarpment in 1923. The new materials expanded the distribution of "*Helaletes*" *mongoliensis* to the Huheboerhe area.

Radinsky (1965a) determined that the lower cheek teeth of "*Helaletes*" *mongoliensis* are more similar to those of *Colodon* in having relatively wider p4–m2 except for the relatively long and narrow p2–3, while the upper cheek teeth are more similar to *Helaletes* (assumed for "*Helaletes*" *intermedius*) in the degree of premolar molarization and proportion of M1, P2–4, except for the more reduced and depressed metacones on M1–3. That Radinsky (1965a) assigned these materials to *Helaletes* rather than to *Colodon* was "an unusually subjective decision" (Radinsky, 1965a: 230).

Dashzeveg and Hooker (1997) erected the genus *Irdinolophus* for "*Helaletes*" *mongoliensis*, and reported an isolated upper preultimate molar of the species from eastern Gobi, Mongolia. They considered *Irdinolophus* as the most primitive member of the family Deperetellidae, because its p3–4 talonid is slightly wider and p4 trigonid shorter than other species of the family; in addition, its p3 paraconid is distinct and premolars show initial elongation (fig. 5C, D). These characters typify advanced members of the Deperetellidae, but they differ from those of *Helaletes nanus* and *Desmatotherium intermedius*. Nevertheless, the wider p3–4 talonid is also encountered in *Desmatotherium intermedius* (AMNH FM 12672) (Radinsky, 1963; Schoch, 1984) and *Colodon occidentalis*, and the distinct or weak p3 paraconid is variable as indicated by *Paracolodon fissus* (see above). The p4 trigonid is not as shortened as in *Colodon* and deperetellids, but somewhat intermediate between *Helaletes* and those two groups. Furthermore, the upper cheek teeth of *Teleolophus* are obviously distinguished from those of "*Helaletes*" *mongo-*

liensis in having P2–4 with a protoloph joining the equally developed metaloph a short distance before its lingual end (hypocone), and M1–3 with protoloph, paracone, and metaloph forming an inverted "U" and a metacone greatly reduced. Last, the earliest known deperetellid is from the Arshantan, earlier than Irdinmanhan "*Helaletes*" *mongoliensis* (Radinsky, 1965a; Meng et al., 2007; Wang et al., 2010). As a result, we are skeptical of considering "*Helaletes*" *mongoliensis* the most primitive member of the family Depetellidae, and the main reason for erecting the new genus "*Irdinolophus*" is not tenable. However, another species *Irdinolophus*? *tuiensis* could hold the validity of *Irdinolophus* by its S-shaped ectoloph.

"*Helaletes*" *mongoliensis* is similar to *Paracolodon fissus* in size (table 1, 2; figs. 6–8) and general morphology, and both are from Irdin Manha Formation, Erlian Basin. Radinsky (1965a) even suggests that *Paracolodon fissus* was probably an advanced variant of "*Helaletes*" *mongoliensis*. On the other hand, Radinsky (1965a) shows that P2–4 of *P. fissus* are more advanced than those of *"Helaletes" mongoliensis* in being relatively shorter and wider (figs. 6, 7) and in having the hypocone better separated from the protocone. Furthermore, the new material shows that "*Helaletes*" *mongoliensis* is different from *P. fissus* in having the M2 paracone distally inclined, M3 metacone slightly more lingually depressed (fig. 4A, B, E–G), p2 metaconid more separated from the protoconid, p2–4 buccodistal cingulum more prominent, p3–4 entoconids stronger, cristid obliqua slightly more buccally extended, p4 talonid relatively wider than trigonid, and m3 with slightly larger hypoconulid (fig. 5A–D).

Unfortunately, the skull of "*Helaletes*" *mongoliensis* (AMNH FM 19161) preserves only the preorbital portion (fig. 9), and this part is broken on the skull of *Paracolodon fissus* (IVPP V 22640). However, the long postcanine diastema of "*Helaletes*" *mongoliensis* suggests a relatively long preorbital portion, which contrasts with the relatively short preorbital portion of *Paracolodon fissus* as deduced from a mandible with a complete symphysis (AMNH FM 81802). The infraorbital foramen of "*Helaletes*" *mongoliensis* opens above the posterior end of P4, whereas that of *Paracolodon fissus* opens above the posterior end of P3. Furthermore, in "*Helaletes*" *mongoliensis*, based on the specimens AMNH FM 19161 and AMNH FM 20156E, the lateral border of the lateral trough of the ascending process of the maxilla seems completely composed of the maxilla and close to the anterior border of the orbital, and the facial part of the lacrimal is probably narrow (fig. 9), a condition similar to that of *Helaletes nanus* (AMNH FM 11635). By contrast, in *Paracolodon fissus* (IVPP V 22640), the lateral border of the lateral trough seems composed of the maxilla and lacrimal and prominently separated from the anterior border of the orbital, and the facial part of the lacrimal is probably larger (fig. 2A). Thus, these cranial differences between "*Helaletes*" *mongoliensis* and *Paracolodon fissus* are probably at the genus level.

Compared with *Helaletes nanus*, besides above mentioned characters, "*Helaletes*" *mongoliensis* is further similar to *H. nanus* (AMNH FM 11635) in having a relatively wide and shallow lateral trough, an anterior portion of the maxilla rising upward, the infraorbital foramen opening above the posterior end of P4, P2–4 metaloph weaker compared with protoloph, P4 protoloph extending toward the preparacrista, and the canine relatively large (Radinsky, 1965a). On the other hand, the facial part of "*Helaletes*" *mongoliensis* bears a shallow maxillary fossa

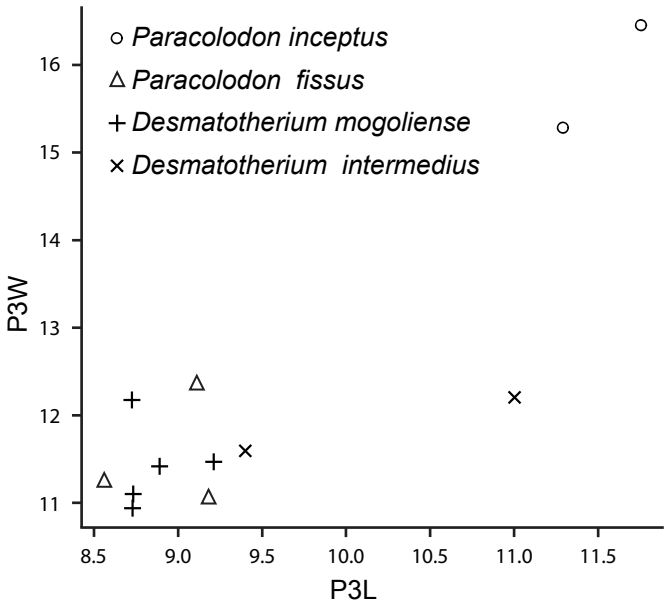

FIG. 6. Scatter plot for P3 size of *Paracolodon* and *Desmatotherium* (in mm).

and a relatively large depression for the attachment of the buccinator muscle above the postcanine diastema, and the canine is closely appressed to the I3 (fig. 9), whereas in *H. nanus* (AMNH FM 11635) the maxillary fossa and depression above the diastema are absent, and the canine is separated from I3 by a diastema. In terms of dentition, "*Helaletes*" *mongoliensis* mainly differs from *Helaletes nanus* in having P2–4 hypocone slightly more separated from the protocone, M1–3 parastyle more closely compressed to paracone, metacone shorter and more lingually depressed, p2–3 entoconid more prominent, talonid relatively wider than trigonid, m1–3 cristid obliqua slightly more reduced, and m3 hypoconulid smaller.

"*Helaletes*" *mongoliensis* is similar to *Desmatotherium intermedius* in having a relatively long postcanine diastema, an infraorbital foramen opening above the posterior border of P4, and a distinct depression for the attachment of the buccinator above the postcanine diastema. They are further similar in having upper cheek teeth relatively long and narrow (figs. 6–8), P2–4 metaloph weaker compared with protoloph, P4 protoloph extending toward preparacrista, M1–3 parastyle compressed to the paracone, metacone less reduced, protoloph and metaloph slightly convex mesially, M2 paracone distally curved, p3–4 talonid wider than trigonid, and entoconid distinct. On the other hand, *Desmatotherium intermedius* is different from "*Helaletes*" *mongoliensis* in having P3–4 somewhat more molariform, M1–3 metacone slightly less lingually depressed, M2–3 centrocrista less aligned with the metaloph, p3–4 talonid relatively wider compared with trigonid, and m3 hypoconulid highly reduced.

In conclusion, considering the differences of cranial characters between *Paracolodon fissus* and "*Helaletes*" *mongoliensis*, and similarities of dental characters and degree of premolar molarization between "*Helaletes*" *mongoliensis* and *Desmatotherium intermedius*, we assigned "*H.*" *mongoliense* to *Desmatotherium* as originally named by Osborn (1923).

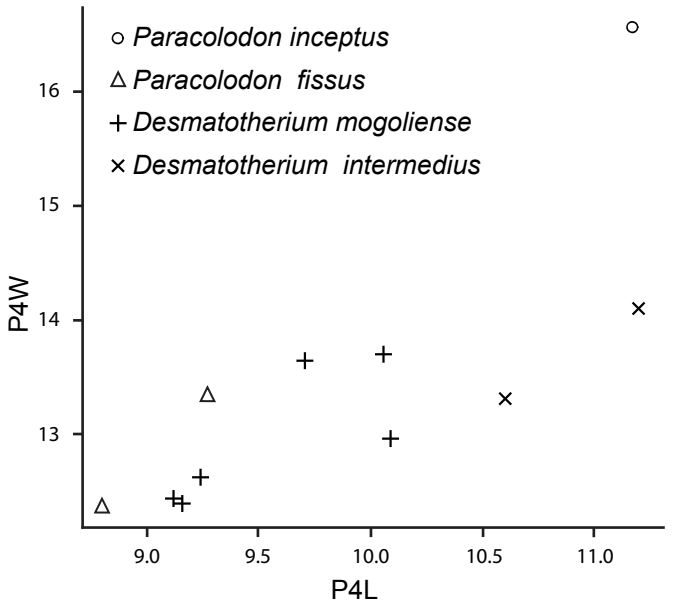

FIG. 7. Scatter plot for P4 size of *Paracolodon* and *Desmatotherium* (in mm).

Radinsky (1965a) also assigned a right lower jaw with p2–m2 (AMNH FM 81803, field no. 927) to *Helaletes* sp. from "Houldjin gravels," 10 miles southwest of Camp Margetts. In fact, this specimen was unearthed from Irdin Manha Formation in Chaganboerhe, where the new material was found (see discussion below). As noted by Radinsky (1965a), the specimen of AMNH FM 81803 is different from *P. fissus* in having "the termination of the symphysis well anterior to p2 and in having relatively long p3–4 trigonids" (Radinsky, 1965a: 231). Furthermore, p3–4 of AMNH FM 81803 has a cristid obliqua buccally extended and a distinct buccodistal cingulum, which suggests its affinity with *Desmatotherium mongoliense*.

Qi (1987) named *Helaletes medius* from the Arshanto Formation, Wulanboerhe, based on fragmental lower jaws (IVPP V 5729, V 5730). However, its specific character of the m1 and m3 having a well-developed cristid obliqua excludes the specimen from Helaletidae, which has a relatively reduced cristid obliqua. On the other hand, the small size, long trigonids of p4–m3, and small hypoconulid on m3 of IVPP V 5729 are very similar to those of AMNH FM 81788 (field no. 931), which was unearthed from Arshanto Formation, 10 miles southwest of Camp Margetts and assigned to *Schlosseria* cf. *S. magister* by Radinsky (1965a). However, the p4–m3 of IVPP V 5729 are relatively wider than those of AMNH FM 81788, and p4 of IVPP V 5729 has a more lingually situated paralophid. The affinity of IVPP V 5729 and the specimens of *Schlosseria* from the Camp Margetts area need further investigation.

HUNTER-SCHREGER BAND (HSB) ANALYSIS

The ectoloph of right P4 of *Paracolodon fissus* and *Desmatotherium mongoliense* were cut longitudinally for the Hunter-Schreger band (HSB) comparison. The studied area of

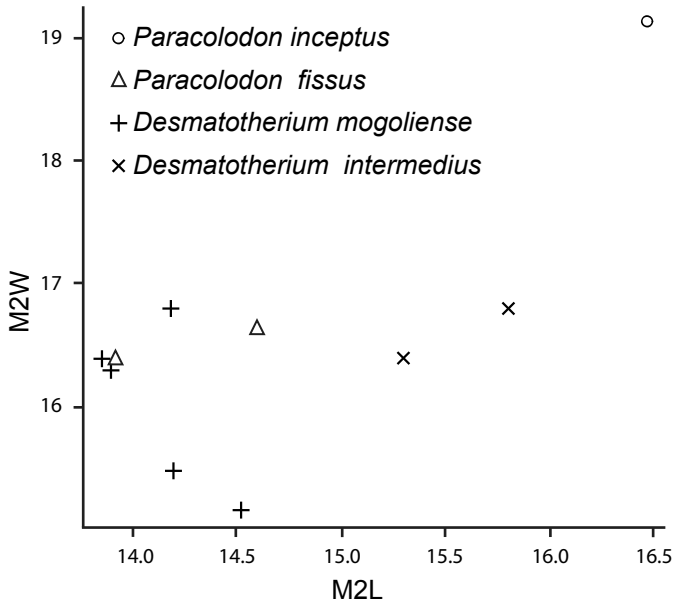

FIG. 8. Scatter plot for M2 size of *Paracolodon* and *Desmatotherium* (in mm).

the two species is characterized by curved HSB with typical interface among cusps indicated by a distinct groove extending almost to the outer enamel surface (fig. 10) (Koenigswald et al., 2011). The HSB curve toward the occlusal surface of the enamel layer and is strictly related to basin areas of the tooth morphology. The curved HSB configuration in both *P. fissus* and *D. mongoliense* confirms the studies by Koenigswald et al. (2011), suggesting their close relationships with helaletids rather than deperetellids, since the latter has a compound HSB configuration (Koenigswald et al., 2011). The HSB pattern in *Desmatotherium* is wave shaped in most areas except in the distal part of the paracone and relatively wide (fig. 10B), whereas those of *Paracolodon* are generally continuous and relatively narrow (fig. 10A).

PHYLOGENETIC ANALYSIS AND ITS IMPLICATIONS

Although the lineage consisting of *Helaletes*, *Desmatotherium*, and *Colodon* was proposed by some authors, it is difficult to assign some specimens to a specific genus based only on dentition, such as *Desmatotherium mongoliense*, *Colodon*? *kayi*, and *Colodon*? *woodi*. The main criteria for the assignments in these groups are premolar characteristics, which are likely to be variable when more than one specimen is available. For instance, in *Desmatotherium mongoliense* the premolar metaloph extends toward either the hypocone or more mesially even to the protocone, the hypocone is variably separated from the protocone, and the metaloph is variable from weak to nearly absent. On the other hand, cranial characters probably play a more important role than dental characters in the study of early tapiroids, considering their characteristic development of a proboscis.

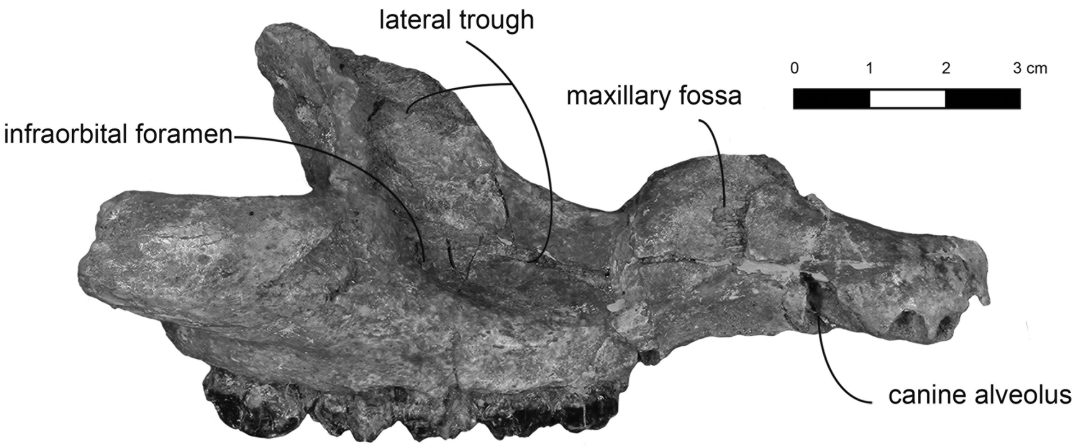

FIG. 9. Anterior cranial portion of *Desmatotherium mongoliense* (AMNH FM 19161).

Colbert (2005, 2006) suggested that *Colodon* is more closely related to *Tapirus* than is *Protapirus*, whereas *Hesperaletes*, *Protapirus*, and *Plesiocolopirus* form a monophyletic group. As discussed above, the skull of *Paracolodon fissus* is different from that of *Colodon occidentalis*, however, it resembles those of *Hesperaletes*, *Protapirus*, and *Plesiocolopirus* in having an anterior sagittal crest extending onto the frontal roof, a lateral trough extending posteriorly over the supraorbital process of the frontal, and a pair of medial troughs on the dorsal surface of the frontal continuing posteriorly to the frontal lines. Besides these three cranial characters, three additional synapomorphic characters of *Hesperaletes*, *Protapirus*, and *Plesiocolopirus* were not preserved on the present skull of *Paracolodon fissus*. These similarities on the skull probably indicate that *Paracolodon* is more closely related to *Hesperaletes*, *Protapirus*, and *Plesiocolopirus* than to *Colodon occidentalis*. However, the differences of teeth and mandible between *Hesperaletes* and *Paracolodon fissus* are distinguishable: the former has a long postcanine diastema, premolars less molariform, upper molar metacone relatively long, slightly less lingually depressed, and slightly convex buccally, metaloph joining the ectoloph mesial to the apex of the metacone, p1 present, lower molars with less reduced cristid obliqua, relatively deep horizontal ramus of the mandible, and the promontory bearing a distinct transpromontorial sulcus (Colbert, 2006).

Cladistic Analyses

We performed phylogenetic analyses using PAUP 4.0 and TNT 1.1 with a parsimony criterion (Swofford, 2002; Goloboff et al., 2008). The heuristic search algorithm was used with 1000 replications of random stepwise addition and tree-bisection-reconnection (TBR) branch swapping. Of the 72 characters, three are parsimony uninformative.

The analyses result in a single most parsimonious tree (fig. 11). The tree length is 268; the consistency index (CI) is 0.4216; the homoplasy index (HI) is 0.5784; the retention index (RI) is 0.5032; the rescaled consistency index (RC) is 0.2122.

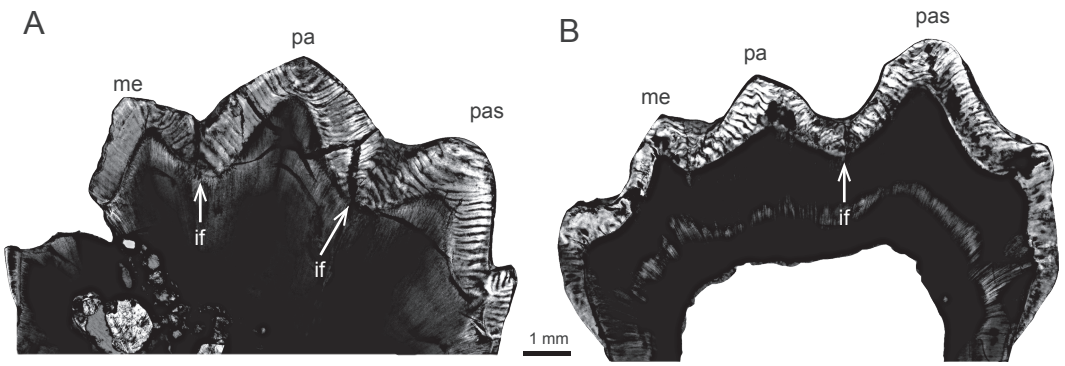

FIG. 10. Longitudinal section of the ectoloph of upper right P4 of *Paracolodon fissus* and *Desmetotherium mongoliense* showing the curved HSB configuration. **A,** *P. fissus* with continuous and relatively narrower HSB pattern; **B,** *D. mongoliens*e with waved and relatively wider HSB pattern. Abbreviations: **if,** interface; **me,** metacone; **pa,** paracone; **pas,** parastyle.

The most parsimonious tree shows some results partially supporting our analyses above. The analysis indicates that both *Paracolodon* and *Colodon* are valid genera. The *Paracolodon* clade (node 20) includes only Asian *P. fissus* and *P. inceptus* and is supported by three synapomorphic characters (appendix 3). The *Colodon* clade (node 25) is supported by four synapomorphic characters (appendix 3), and *Colodon stovalli* is at the base of the clade. The species *C.*? *woodi* and *C.*? *kayi* are also included in *Colodon* clade instead of *Paracolodon*, which is consistent with statements proposed by Radinsky (1963). Nevertheless, the species *C.*? *woodi* and *C.*? *kayi* are more reasonably assigned in either *Colodon* or *Paracolodon* rather than in *Desmatotherium* as originally referred to. Furthermore, the result shows *Paracolodon* and *Colodon* form a sister group, which indicates that *Paracolodon* is more closely related to *Colodon* than to *Hesperaletes*, *Protapirus*, or *Plesiocolopirus*, in contrast to the above analysis based on cranial characters. The *Paracolodon-Colodon* clade (node 26) is supported by four synapomorphic characters (appendix 3). *Plesiocolopirus* and *Protapirus* form successive sister-taxa lineages to *Paracolodon-Colodon* clade. The high-latitude late Wasatchian *Thuliadanta mayri* is more primitive than *Helaletes* (Eberle, 2005), and they form successive sister-taxa lineages to *Plesiocolopirus*, *Protapirus*, *Colodon*, and *Paracolodon* clade. Furthermore, the result also supports that the assignment of the species *Desmatotherium mongoliense* and *Paracolodon fissus* from Irdin Manha Formation, Erlian Basin, into two different genera, since *Desmatotherium mongoliense* and *Desmatotherium intermedius* form a sister group that is more closely related to *Heteraletes* than to any other helaletids. The *Desmatotherium* clade (node 31) is supported by six synapomorphic characters (appendix 3). *Hesperaletes* is placed in a relatively basal position, more derived than *Heptodon* but less derived than any other helaletids. To sum up, the result of the cladistic analysis is partially consistent with the results based on the morphologic comparisons, although some discrepancies are present. It is premature to resolve these discrepancies considering the lack of cranial materials for many helaletids.

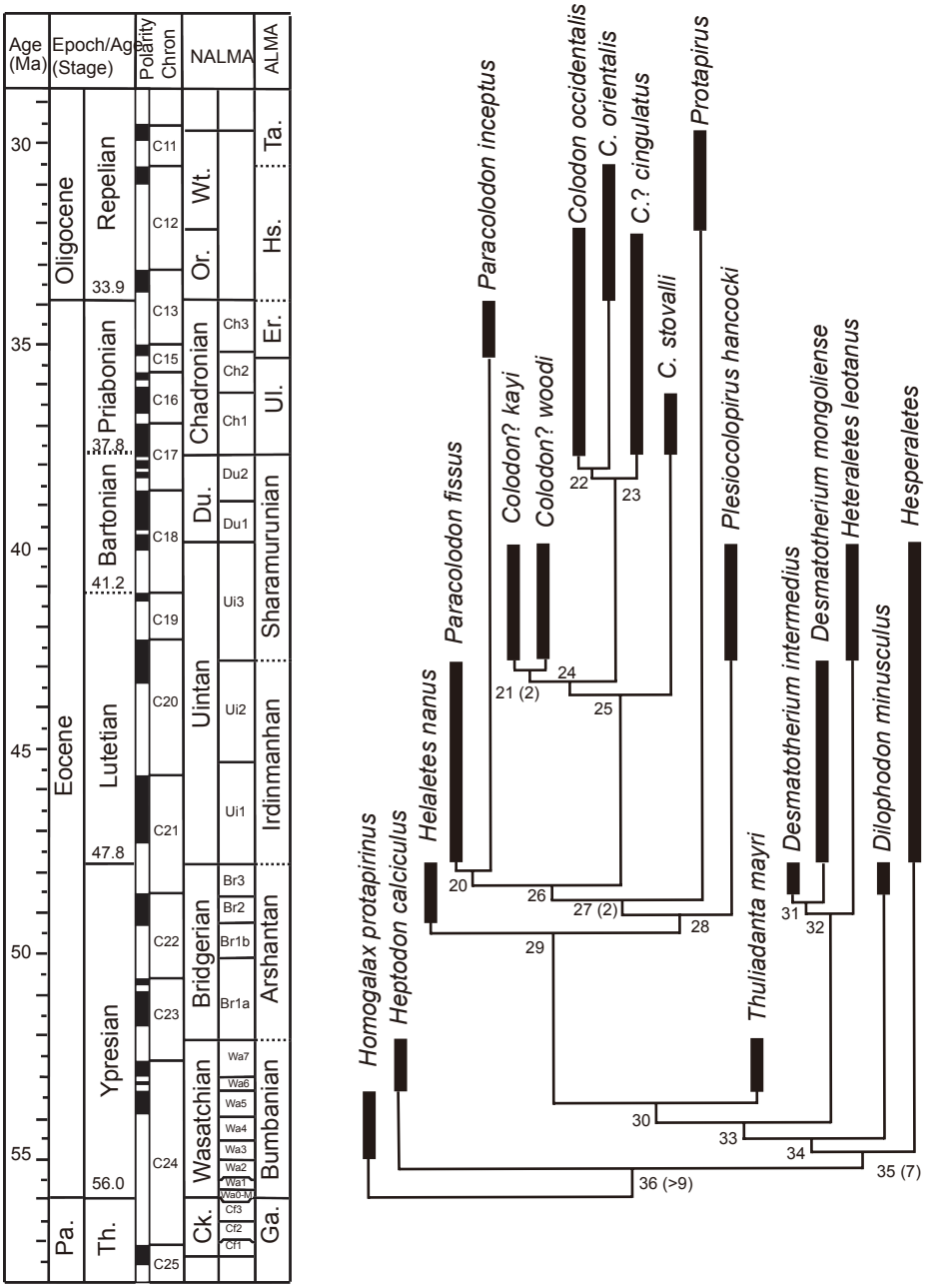

FIG. 11. The single most parsimony tree and the distribution of selected taxa. The left column showing Polarity Chrons, NALMA, and ALMA was modified from Vandenberghe et al. (2012). Numbers on the cladogram are node numbers, and numbers in the parentheses are Bremer Support which is greater than 1. Abbreviations: **ALMA,** Asian Land Mammal Ages; **Ck.,** Clarkforkian; **Du.,** Duchesnean; **Er.,** Ergilian; **Ga.,** Gashatan; **Hs.,** Hsandagolian; **NALMA,** North American Land Mammal Ages; **Or.,** Orellan; **Pa.,** Paleocene; **Ta.,** Tabenbulakian; **Th.,** Thanetian; **Ul.,** Ulangochuian; **Wt.,** Whitneyan.

Irdinmanhan ALMA

The phylogenetic analysis combined with morphological comparisons is also informative for correlation between Irdinmanhan ALMA (Asian Land Mammal Ages) and related NALMA (North American Land Mammal Ages). The Irdinmanhan ALMA is commonly correlated to the Uintan NALMA, but precise correlation is not clear (Romer, 1966; Vandenberghe et al., 2012). Tong et al. (1995) suggested that Irdinmanhan should be correlated with early Uintan, whereas the late Uintan is equal to Sharamurunian ALMA. Ni et al. (2010) suggested that the Irdinmanhan is probably slightly older than Ui1 subage of the Uintan, based on the fact that *Tarkops* from the Irdin Manha Formation is more primitive than *Tarka* from Ui1. The rodent assemblage (Li, 2016) from the lower part of the Irdin Manha Formation also suggested that the Irdinmanhan may be earlier than late Eocene and should be correlated with early Uintan (Li and Meng, 2015).

The Ulan Shireh fauna in the Shara Murun region has been roughly correlated to the Irdin Manha fauna (Radinsky, 1965a, 1967; Ye, 1983; Wang et al., 2012), but Li et al. (2016) recognized a most probably Sharamurunian of the upper horizon of the Ulan Shireh Formation. To better define the Irdin Manha fauna, we list the following perissodactyls that are exclusively from the Irdin Manha Formation at the Irdin Manha escarpment and Huheboerhe area where the Irdin Manha Formation is well identified. These perissodactyls include: Brontotheriidae: *Microtitan mongoliensis*, *Protitan grangeri* (= *P. robustus*, *P. obliquidens*), *Protitan minor*, *Protitan*? *cingulatus*, *Gnathotitan berkeyi*, *Metatitan relictus*, *Hyotitan thomsoni*, *Metatelmatherium cristatum*, *Metatelmatherium parvum*; Deperetellidae: *Teleolophus medius*, *Deperetella* sp.; Helaletidae: *Paracolodon fissus*, *Desmatotherium monogoliense*; Lophialetidae: *Lophialetes expeditus*; Hyracodontidae: *Triplopus*? *proficiens*, Paraceratheriidae *Fostercooperia totadentata*, Amynodontidae *Rostriamynodon grangeri* (Granger and Gregory, 1943; Radinsky, 1965a, 1967; Russell and Zhai, 1987; Wall and Manning, 1986; Mihlbachler, 2008). Lophialetidae and Deperetellidae are endemic families in Asia, and many brontotheres are indigenous (Granger and Gregory, 1943; Radinsky, 1965a). Among brontotheres, *Metatelmatherium cristatum* was considered as a junior synonym of the Uintan *Metatelmatherium ultimum* from North America (Mihlbachler, 2008). Among hyracodontids, the North American *Triplopus* had a temporal distribution ranging from the Uintan to Duchesnean, and *Uintaceras*, which is similar to *Fostercooperia* to some extent, is from the Uintan (Radinsky, 1967; Holbrook and Lucas, 1997; Prothero, 1998). On the other hand, *Rostriamynodon* was considered more primitive than the Uintan *Amynodon* from North America (Wall and Manning, 1986).

Among helaletids from the Erlian Basin, *Paracolodon fissus* is more primitive than *C.*? *kayi* and *C.*? *woodi* from late Uintan Sage Creek, Montana, and Wind River Basin, Wyoming (Radinsky, 1963), in degree of premolar molarization, and thus supports a probable date for the Irdinmanhan earlier than late Uintan (fig. 11). Furthermore, upper molars of *Desmatotherium mongoliense* from Irdin Manha Formation are slightly more derived than those of *D. intermedius* from the late Bridgerian of the Bridger Basin and probably Washakie Basin, Wyoming (Radinsky, 1963; Schoch, 1984); thus, the Asian Irdinmanhan is probably younger than the late Bridgerian. Based on all available evidence, we suggest that the Irdinmanhan can be restricted in the interval roughly correlative to Ui1 and Ui2 subages of the North Amerian Uintan (fig. 11).

COMMENTS ON THE LOCALITIES IN HUHEBOERHE (CAMP MARGETTS) AREA

The holotype of *Paracolodon fissus* (AMNH FM 20161, field no. 147) was collected from Irdin Manha beds, Camp Margettes, 25 miles southwest of Iren Dabasu in 1923 (Granger, 1923, p. 9). Radinsky (1965a) referred two mandibles to *P. fissus*?. One specimen came from the "Irdin Manha" beds (AMNH FM 81802, field no. 865) and the other from "Houldjin gravels" (AMNH FM 81804, field no. 839) at Camp Margetts; both were collected by CAE in 1930. Recent works have clarified that the Camp Margetts site was near the Duheminboerhe locality, and the "Houldjin gravels" and "Irdin Manha" beds in the Camp Margetts area are considered equivalent to the Irdin Manha Formation and Arshanto Formation, respectively (Meng et al., 2007; Sun et al., 2009; Wang et al., 2010; Wang et al., 2012). Nevertheless, reexamining the original CAE field notes and specimens, we found that the type specimen of *P. fissus* was actually from the Irdin Manha Formation. The field notes documented that the specimen was from "white to gray arkosic, concretionary sandstones and conglomerates contain chief fossil horizons" on the stretch at "mile 24.6" (Morris, 1923: 79; see also Meng, 1990: fig. 4A). From our field experience in the area, we suspect that the field number 147, where the holotype of *P. fissus* was found, was around the site of "24.6 miles" ("best fossils" as shown on Morris's sketch) rather than "25 miles" of Iren Dabasu, as recorded by Granger (1930). The preservation condition of *P. fissus* holotype is similar to the specimen AMNH FM 81804; both have white bones and dark teeth. A similar condition is seen in the new specimen of *D. mongoliense* (IVPP V 14692) from the base of Irdin Manha Formation, Changanboerhe. The specimen AMNH FM 81802, although recorded from "Irdin Manha Formation," has dark gray bone and teeth, which is similar to the condition of IVPP V 22640, but different from specimens of the underlying Arshanto Formation. Thus, we think that all known specimens of *P. fissus* were from the Irdin Manha Formation at today's Duheminboerhe.

We also think that some specimens collected from the "Irdin Manha Formation" near Camp Margetts were indeed from Irdin Manha Formation. For instance, *Metatelmatherium cristatum* (AMNH FM 26411) from Camp Margetts, *Protitian minor* (AMNH FM 26416) from 0.5 mile west of Camp Margetts, and *Rostriamynodon grangeri* from 2 miles east of Camp Margetts were all recorded from "Irdin Manha Formation," although the matrix associated with the specimens is gray sandstone and gravel comparable with that of the Irdin Manha Formation instead of the Arshanto Formation in this area. There is no doubt that specimens of *Dematotherium mongoliensis* were collected from the Irdin Manha Formation of the Irdin Manha escarpment and Huheboerhe area.

After a short visit to the locality 24.6 miles southwest of Iren Dabasu in the year 1923, CAE returned to that locality in the year 1930. CAE named the locality "Camp Margetts" in honor of a guest, a Lieutenant-Colonel N.E. Margetts, and made more comprehensive collections in that area and nearby localities (from early August to late September) (Andrews, 1932; Granger, 1930). The place named "Camp Margetts" is a vital location, because it serves as an anchor locality from which other sites were named and distances and directions defined; however, the specific location of Camp Margetts and its related sites had been uncer-

tain and controversial for many years (Radinsky, 1964; Qi, 1987). Based on the sketches of sections in CAE field books and lithological characters, Meng (1990) first correctly pointed out that "Camp Margetts" was located in Duheminboerhe, and the localities identified in the field books as 6 miles west, 7 miles west and southwest, and 10 miles southwest of "Camp Margetts" were located along the Huheboerhe escarpment. After more detailed fieldwork in recent years, Meng et al. (2007) and Wang et al. (2010, 2012) further demonstrated that the locality 6 miles west of Camp Margetts is Nuhetingboerhe, that 7 miles southwest of Camp Margetts is Wulanboerhe, and that 10 miles southwest of Camp Margetts is Huheboerhe, while the locality 5 miles east of Camp Margetts (described as an "overnight camp" in the field books) is Daoteyin Obo. Meng et al. (2007) also considered the locality 7 miles southwest to be the same as that 7 miles west. By contrast, Wang et al. (2010, 2012) considered the locality 7 miles southwest and the one described as 7 miles west of Camp Margetts should be different localities, the former Wulanboerhe, and the latter a place in the north of Wulanboerhe. Nevertheless, the exact location of Camp Margetts is not clear, and the distances between Nuhetingboerhe, Wulanboerhe, and Huheboerhe to Camp Margetts seem considerably less than 6 miles, 7 miles southwest, and 10 miles southwest, respectively, especially for the last two localities. The solution to these questions is essential, because many holotypes of mammalian fossils were discovered in these localities by CAE.

Morris's sketch (Morris, 1923: 76) shows that the section at 24.6 miles is on the west side and very close to a road (fig. 12). Eight years later, Granger's sketch (1930: 22) showed that Camp Margetts is also very close to the same road from Iren Dabasu to Sair Usu (see also Meng, 1990: fig. 3), but somewhat farther to the west. Both of the sketches show that the road passes an angled profile between the northern lowland and southern upland, where it was labeled as 25 miles on Morris's sketch (fig. 12). Such a road is probably near the road from Duheminhuduge to Erlian on the present topographic map (fig. 1). The sketch at 24.6 miles by Morris is relatively steep and thick (Meng, 1990: fig. 4A), which is consistent with the stratigraphic section on west side of the present road. The sketch and the stratigraphic section are also similar in lithology. By contrast, the section becomes more gradual and much thinner on the south side of the road. Furthermore, on Morris's sketch there is a prominent notch on the east of the angled profile, and another escarpment is about 5 miles east (fig. 12) (see also Morris, 1923, Book 2, p. 35). Such a notch is consistent with the lowland between Duheminboerhe and Daoteyin Obo, and the distance between them is also about 5 miles (fig. 1). This shows that today's road from Duheminhuduge to Erlian is very close to the one mapped by Morris and Granger from Iren Dabasu to Sair Usu (figs. 1, 8). According to the field book of Granger (1930), it is clear that Camp Margetts is located on the west side of Morris's "25 miles" locality. Furthermore, many fossils were collected from the west side of Camp Margetts (0.5 miles west, 1 mile west, and 1.5 miles west), whereas only one locality 2 miles east of Camp Margetts was recorded, bearing only two field numbers (890 and 921), besides the Daoteyin Obo (overnight camp). We thus infer that Camp Margetts should be located on the west side of the point where the road intersects the upland, and closer to east than to west rim of the Duheminboerhe escarpment (fig. 1).

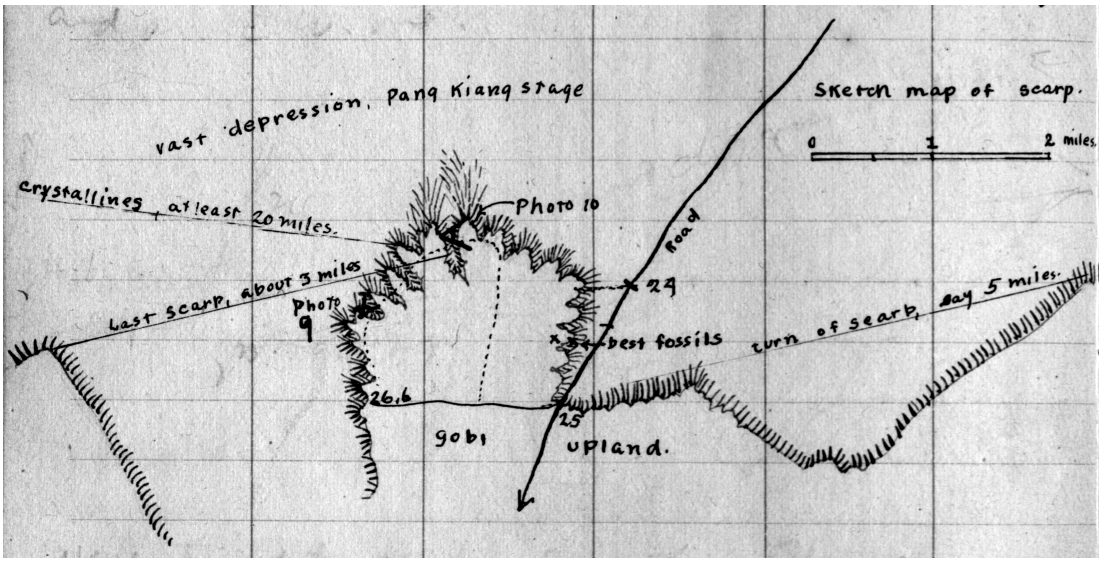

FIG. 12. Sketch map of the locality later named as Camp Margetts (Moriss, 1923, vol. 2: 76).

Meng et al. (2007) considered that the locality 7 miles (235°) southwest of Camp Margetts is the same as the locality 7 miles west of Camp Margetts. We agree with their notation and consider the locality 7 miles southwest (235°) of Camp Margetts is more accurate. Only two specimens of *Advenimus burkei* (field no. 892) were listed from 7 miles, 235°, whereas the successive pages of Granger's field book in 1930 he recorded all fossils from "7 miles west." At that locality, CAE conducted fieldwork for more than two weeks (about from Aug. 30–Sept. 16) and collected a large number of fossils. We think that the locality Granger named as "7 miles west" of Camp Margetts is actually the locality known as "7 miles, 235°" (agreeing with Meng et al., 2007) but is Huheboerhe rather than Wulanboerhe (fig. 1) for the following reasons: (1) The distance between Huheboerhe and Camp Margetts is about 7 miles (11.3 km), while that of Wulanboerhe and Camp Margetts is only about 6 miles (9.7 km). (2) Granger's sketch map at 7 miles southwest (235°) of Camp Margetts (Granger, 1930, 38; Meng et al., 2007: fig. 6) has relatively thick "Houldjin" and "gray clays" of "Irdin Manha," which bears many specimens of "*Eudinoceras*" (latter identified as *Gobiatherium*) from the basal strata. Meng et al. (2007) considered "Houldjin" equivalent to "Irdin Manha" and bed 12 of the section of Meng et al. (2004); "gray clays" of "Irdin Manha" correlated with basal Arshato Formation of Nuhetingboerhe; and the underlying "Red Clays" and "Gray and reddish clays" corresponded to the Nomogen Formation. However, Meng et al. (2007) did not distinguish the "gray clays" of "Irdin Manha" from the Wulanboerhe section. Actually, at Wulanboerhe bed 12 of Meng et al. (2004) should be the Arshanto Formation, which is relatively thinner at that site, whereas all the underlying beds are Nomogen Formation. (3) At 7 miles, 235°, of Camp Margetts, the CAE collected a large number of fossils both from "Irdin Manha" and "Houldjin" formations; however, none of the Paleogene mammals were recorded from there. In contrast, at Wulanboerhe the fossils were mainly from the Nomogen Formation and the basal Arshanto Formation that generated char-

acteristic late Paleocene and early Eocene taxa, while the Irdinmanhan mammals were absent. *Eudinoceras mongoliensis*, *Gobiatherium mirificum*, "*Helaletes medius*", *Teleolophus primarius*, *Teleolophus*? *rectus*, and *Mesonyx uqbulakensis* were reported from the basal Arshanto Formation at Wulanboerhe (Qi, 1987; Lucas, 2001; Bai, 2006; Jin, 2012; Mao and Wang, 2012). (4) One specimen of typical Arshantan *Gobiatherium mirficum* (AMNH FM 26637, field no. 910) was recorded from the "top of the red clays which underlies the upper gray clays" (Granger, 1930: 46; Lucas, 2001; Bai, 2006), which is inconsistent with a correlation between the "red clays" and the Nomogen Formation at Wulanboerhe.

As a result, we consider the locality dubbed 7 miles southwest (235°) of Camp Margetts is Huheboerhe instead of Wulanboerhe. Thus, all specimens collected by CAE from 7 miles west of Camp Margetts are actually from Huheboerhe. The "Houldjin" is equivalent to the Irdin Manha Formation, and all the underlying beds are Arshanto Formation. The "gray clays" bearing lots of *Gobiatherium mirificum* is correlated with bed 8 of the section of Meng et al. (2007). Obviously, CAE did not recognize the Nomogen Formation, nor even the basal Arshanto Formation, at the base of the section.

In the year 2013, the present authors investigated another locality, Chaganboerhe, which is in the south of the Huheboerhe escarpment (fig. 1). The stratigraphy at this site is similar to that of Huheboerhe and also rich in fossil mammals (Meng et al., 2007, fig. 7). More importantly, its distance to Camp Margetts is approximate 10 miles southwest. We think the locality described as 10 miles southwest of Camp Margetts is actually Chaganboerhe, where CAE spent about one week for excavation (from Sept. 16 to Sept. 22) (Granger, 1930). Detailed comparisons between Chaganboerhe and "10 miles southwest of Camp Margetts" need further investigation. Granger (1930: 53) probably erroneously recorded the field no. 923 specimen (AMNH FM 26414, brontothere) at 10 miles west of Camp Margetts; the real provenance is more likely from 10 miles southwest of Camp Margetts, because at 10 miles west of the latter there is no outcrop.

Finally, Meng et al. (2007) considered the locality 6 miles west of Camp Margetts to be Nuhetingboerhe, and we generally agree with that assessment. It should be noted that only the last two days (Sept. 25–26) of the whole CAE were spent 6 miles west of Camp Margetts, and *Eudinoceras mongoliensis* (field nos. 934, 935, 937) and *Litolophus gobiensis* (field no. 936) were collected from there (Granger, 1930). More specifically, we think that the locality 6 miles west of Camp Margetts is closer to "chalicothere pit," which is located a short distance south of the main Nuhetingboerhe section.

ACKNOWLEDGMENTS

We thank Qian Li, Xun Jin, Haibing Wang, Wei Zhou, Shijie Li, Qi Li, Yongxing Wang, Yongfu Wang, Yan Li, Wei Chen, Qiang Cao, Qiang Li, Baohua Sun (all IVPP), K. C. Beard (University of Kansas), and D. L. Gebo (Northern Illinois University) for assistance in the field; Wei Zhou, Shijie Li, and Qi Li (all IVPP) for preparation of specimens. We thank R. O'Leary, J. Galkin, A. Gishlick, C. Mehling, L. Jurgielewicz (all AMNH), A. Henrici and A. Tabrum

(both Carnegie Museum of Natural History), P. Gingerich and A. Rountrey (both Museum of Paleontology, University of Michigan), C. Norris and D. Brinkman (both Yale Peabody Museum of Natural History) for access to the specimens in their care; A. Balcarcel, R. Evander, V. Lee, A. Davidson (all AMNH), A. Tabrum (Carnegie Museum of Natural History), and M. Fox (Yale Peabody Museum of Natural History) for providing the comparative casts; S. Bell, T. Baione, M. Reitmeyer, and A. Springer (all AMNH) for providing the access and help to the literatures and CAE field notes at the AMNH. Discussion with M. O'Leary (Stony Brook University) on petrosals greatly benefited the first author. We are grateful to Z.J. Tseng (University at Buffalo, State University of New York) for improving English text and comments of the manuscript. We thank T. Simth (Royal Belgian Institute of Natural Scienc), editor R.S. Voss (AMNH), and an anonymous reviewer for critical and helpful comments, and M. Knight (AMNH) for instructive editoral comments. We thank the Bureau of Land and Resources of Erlian, Inner Mogolia for the support. Funding was provided by grants from China Scholarship Council, Frick Funds from the Division of Paleontology, American Museum of Natural History, Chinese Academy of Sciences (KZCX22EW2106), National Basic Research Program of China (973 Program) (2012CB821900), the National Natural Science Foundation of China (41002009, 41672014, 41572021, 41404022), the Special Fund for Fossil Excavation and Preparation, CAS, the China Geological Survey (Nos. 1212011120115 and 1212011120142), State Key Laboratory of Palaeobiology and Stratigraphy (Nanjing Institute of Geology and Palaeontology, CAS) (No.163103), and Youth Innovation Promotion Association, CAS.

REFERENCES

Andrews, R.C. 1932. The new conquest of Central Asia. *In* Natural history of Central Asia, vol. 1: 1–678. New York: American Museum of Natural History.

Bai, B. 2006. New materials of Eocene Dinocerata (Mammalia) from the Erlian Basin, Nei Mongol (Inner Monogolia). Vertebrata PalAsiatica 44 (3): 250–261.

Bai, B., Y.Q. Wang, and J. Meng. 2010. New craniodental materials of *Litolophus gobiensis* (Perissodactyla, "Eomoropidae") from Inner Mongolia, China, and phylogenetic analyses of Eocene chalicotheres. American Museum Novitates 3688: 1–27.

Bai, B., Y.Q. Wang, J. Meng, Q. Li, and X. Jin. 2014. New Early Eocene basal tapiromorph from southern China and its phylogenetic implications. Plos One 9 (10): e110806.

Borissiak, A. 1918. On the remains of a lophiodontoid ungulate from the Oligocene deposits of Turgai. Annales de la Société Paléontologique Russie 2: 27–31.

Cifelli, R.L. 1982. The petrosal structure of *Hyopsodus* with respect to that of some other ungulates, and its phylogenetic implications. Journal of Paleontology 56 (3): 795–805.

Colbert, M.W. 2005. The facial skeleton of the early Oligocene *Colodon* (Perissodactyla, Tapiroidea). Palaeontologia Electronica 8 (1): 1–27.

Colbert, M.W. 2006. *Hesperaletes* (Mammalia: Perissodactyla), a new tapiroid from the middle Eocene of southern California. Journal of Vertebrate Paleontology 26 (3): 697–711.

Colbert, M.W., and R.M. Schoch. 1998. Tapiroidea and other moropomorphs. *In* C.M. Janis, K.M. Scott, and L.L. Jacobs (editors), Evolution of Tertiary mammals of North America: 569–582. Cambridge: Cambridge University Press.

Cooper, L.N., et al. 2014. Anthracobunids from the Middle Eocene of India and Pakistan are stem perissodactyls. PLoS One 9 (10): e109232.

Dashzeveg, D., and J.J. Hooker. 1997. New ceratomorph perissodactyls (Mammalia) from the Middle and Late Eocene of Mongolia: their implications for phylogency and dating. Zoological Journal of the Linnean Society 120: 105–138.

Eaton, J.G. 1985. Paleontology and correlation of the Eocene Tepee Trail and Wiggins formations in the north fork of Owl Creek area, southeastern Absaroka Range, Hot Springs County, Wyoming. Journal of Vertebrate Paleontology 5 (4): 345–370.

Eberle, J.J. 2005. A new "tapir" from Ellesmere Island, Arctic Canada—implications for northern high latitude palaeobiogeography and tapir palaeobiology. Palaeogeography Palaeoclimatology Palaeoecology 227 (4): 311–322.

Gazin, C.L. 1956. The geology and vertebrate paleontology of upper Eocene strata in the northeastern part of the Wind River Basin, Wyoming. Part 2. The mammalian fauna of the Badwater Area. Smithsonian Miscellaneous Collection 131 (8): 1–35.

Goloboff, P.A., J.S. Farris, and K.C. Nixon. 2008. TNT, a free program for phylogenetic analysis. Cladistics 24: 774–786.

[Granger, W.] 1923. [Records of fossils collected in Mongolia.] Central Asiatic Expeditions. Field books of the Third Asiatic Expedition. RBC51D. American Museum of Natural History Library: 1–73.

[Granger, W.] 1930. [Records of fossils collected in Mongolia.] Central Asiatic Expeditions. Field books of the Third Asiatic Expedition. RBC51E. American Museum of Natural History Library: 1–57, 160–163.

Granger, W., and W.K. Gregory. 1943. A revision of the Mongolian titanotheres. Bulletin of American Museum of Natural History 80 (10): 349–389.

Holbrook, L.T. 2009. Osteology of *Lophiodon cuvier*, 1822 (Mammalia, Perissodactyla) and its phylogenetic implications. Journal of Vertebrate Paleontology 29 (1): 212–230.

Holbrook, L.T., and S.G. Lucas. 1997. A new genus of rhinocerotoid from the Eocene of Utah and the status of North American "*Forstercooperia*." Journal of Vertebrate Paleontology 17 (2): 384–396.

Holbrook, L.T., S.G. Lucas, and R.J. Emry. 2004. Skulls of the Eocene perissodactyls (Mammalia) *Homogalax* and *Isectolophus*. Journal of Vertebrate Paleontology 24 (4): 951–956.

Hooker, J.J. 1984. A primitive ceratomorph (Perissodactyla, Mammalia) from the Early Tertiary of Europe. Zoological Journal of the Linnean Society 82 (1–2): 229–244.

Hooker, J.J. 1989. Character polarities in early Eocene perissodactyls and their significance for *Hyracotherium* and infraordinal relationships. *In* D.R. Prothero and R.M. Schoch (editors), The evolution of perissodactyls: 79–101. New York: Oxford University Press.

Hooker, J.J. 2005. Perissodactyla. *In* Rose, K.D., and J.D. Archibald (editors), The rise of placental mammals: origins and relationships of the major extant clades: 199–214. Baltimore: Johns Hopkins University Press.

Hooker, J.J. 2010. The mammal fauna of the early Eocene Blackheath Formation of Abbey Wood, London. Monograph of the Palaeontographical Society 164 (634): 1–157.

Hooker, J.J., and D. Dashzeveg. 2004. The origin of chalicotheres (Perissodactyla, Mammalia). Palaeontology 47: 1363–1386.

Hough, J. 1955. An Upper Eocene Fauna from the Sage Creek Area, Beaverhead County, Montana. Journal of Paleontology 29 (1): 22–36.

Jin, X. 2012. New mesonychid (Mammalia) material from the lower Paleogene of the Erlian Basin, Nei Mongol, China. Vertebrata PalAsiatica 50 (3): 245–257.

Kapur, V.V., and S. Bajpai. 2015. Oldest South Asian tapiromorph (Perissodactyla, Mammalia) from the Cambay Shale Formation, western India, with comments on its phylogenetic position and biogeographic implications. Palaeobotanist 64: 95–103.

Koenigswald, W. von, L.T. Holbrook, and K.D. Rose. 2011. Diversity and evolution of Hunter-Schreger band configuration in tooth enamel of perissodactyl mammals. Acta Palaeontologica Polonica 56 (1): 11–32.

Li, P., and Y.Q. Wang. 2010. Newly discovered *Schlosseria magister* (Lophialetidae, Perissodactyla, Mammalia) skulls from central Nei Mongol,China. Vertebrata PalAsiatica 48 (2): 119–132.

Li, Q. 2016. Eocene fossil rodent assemblages from the Erlian Basin (Inner Mongolia, China): biochronological implications. Palaeoworld 25 (1): 95–103.

Li, Q., and J. Meng. 2015. New ctenodactyloid rodents from the Erlian Basin, Nei Mongol, China, and the phylogenetic relationships of Eocene Asian ctenodactyloids. American Museum Novitates 3828: 1–58.

Li, Q., Y.Q. Wang, and L. Fostowicz-Frelik. 2016. Small mammal fauna from Wulanhuxiu (Nei Mongol, China) implies the Irdinmanhan-Sharamurunian (Eocene) faunal turnover. Acta Palaeontologica Polonica 61 (4): 759–776.

Lucas, S.G. 2001. *Gobiatherium* (Mammalia: Dinocerata) from the middle Eocene of Asia: taxonomy and biochronological significance. Palaontologische Zeitschrift 74 (4): 591–600.

Mader, B.J. 2009. Details of the cranial anatomy of a primitive diplacodont brontothere, cf. *Protitanotherium*, from the Wiggins Formation of Wyoming (Mammalia, Perissodactyla, Brontotheriidae). Journal of Vertebrate Paleontology 29 (4): 1224–1232.

Matthew, W.D., and W. Granger. 1925a. New ungulates from the Ardyn Obo Formation of Mongolia with faunal list and remarks on correlation. American Museum Novitates 195: 1–12.

Matthew, W.D., and W. Granger. 1925b. The smaller perissodactyls of the Irdin Manha Formation, Eocene of Mongolia. American Museum Novitates 199: 1–9.

McKenna, M.C., and S.K. Bell. 1997. Classification of mammals above the species level. New York: Columbia University Press.

Mao, F.Y., and Y.Q. Wang. 2012. Coryphodontids (Mammalia: Pantodonta) from the Erlian Basin of Nei Mongol, China, and their biostratigraphic implications. Vertebrata PalAsiatica 50 (3): 258–280.

Meng, J. 1990. A new species of Didymoconidae and comments on related locality and stratigraphy. Vertebrata PalAsiatica 28 (3): 206–217.

Meng, J., et al. 2004. *Gomphos elkema* (Glires, Mammalia) from the Erlian Basin: evidence for the early Tertiary Bumbanian land mammal age in Nei-Mongol, China. American Museum Novitates 3425: 1–24.

Meng, J., et al. 2007. New stratigraphic data from the Erlian Basin: Implications for the division, correlation, and definition of Paleogene lithological units in Nei Mongol (Inner Mongolia). American Museum Novitates 3570: 1–31.

Mihlbachler, M.C. 2008. Species taxonomy, phylogeny, and biogeography of the Brontotheriidae (Mammalia: Perissodactyla). Bulletin of the American Museum of Natural History 311: 1–475.

Morris, F.K. 1923. [Central Asiatic expeditions.] Field books of the Third Asiatic Expedition. Book 2. RBC51D. American Museum of Natural History Library.

Ni, X.J., et al. 2010. A new tarkadectine primate from the Eocene of Inner Mongolia, China: phylogenetic and biogeographic implications. Proceedings of the Royal Society B, Biological Sciences 277 (1679): 247–256.

O'Leary, M.A. 2010. An anatomical and phylogenetic study of the osteology of the petrosal of extant and extinct artiodactylans (Mammalia) and relatives. Bulletin of the American Museum of Natural History 335: 1–206.

O'Leary, M.A., et al. 2013. The placental mammal ancestor and the post-K-Pg radiation of placentals. Science 339 (6120): 662–667.

Osborn, H.F. 1923. Titanotheres and lophiodonts in Mongolia. American Museum Novitates 91: 1–5.

Prothero, D.R. 1998. Hyracodontidae. *In* C.M. Janis, K.M. Scott, and L.L. Jacobs (editors), Evolution of Tertiary mammals of North America: 589–594. Cambridge: Cambridge University Press.

Qi, T. 1987. The Middle Eocene Arshanto fauna (Mammalia) of Inner Mongolia. Annals of Carnegie Museum 56: 1–73.

Radinsky, L. 1963. Origin and early evolution of North American Tapiroidea. Peabody Museum of Natural History, Yale University 17: 1–106.

Radinsky, L.B. 1964. Notes on Eocene and Oligocene fossil localities in Inner Mongolia. American Museum Novitates 2180: 1–11.

Radinsky, L.B. 1965a. Early Tertiary Tapiroidea of Asia. Bulletin of American Museum of Natural History 129 (2): 181–263.

Radinsky, L.B. 1965b. Evolution of the tapiroid skeleton from *Heptodon* to *Tapirus*. Bulletin of the Museum of Comparative Zoology 134 (3): 69–106.

Radinsky, L.B. 1967. A review of the rhinocerotoid family Hyracodontidae (Perissodactyla). Bulletin of American Museum of Natural History 136 (1): 1–46.

Romer, A.S. 1966. Vertebrate paleontology. Chicago: University of Chicago Press.

Rose, K.D., et al. 2014. Early Eocene fossils suggest that the mammalian order Perissodactyla originated in India. Nature Communications 5 (5570): 1–9.

Russell, D.E., and R.J. Zhai. 1987. The Palaeogene of Asia: mammals and stratigraphy. Mémoires du Muséum National d'Histoire Naturelle, Sciences de la Terre (Series C) 52: 1–488.

Savage, D.E., D.E. Russell, and P. Louis. 1965. European Eocene Equidae (Perissodactyla). University of California Publications on Geological Science 56: 1–94.

Schoch, R.M. 1984. Two unusual specimens of *Helaletes* in the Yale Peabody Museum collections, and some comments on the ancestry of the Tapiridae (Perissodactyla, Mammalia). Postilla 193: 1–20.

Schoch, R.M. 1989. A review of the tapiroids. *In* D.R. Prothero, and R.M. Schoch (editors), The evolution of perissodactyls: 298–320. New York: Oxford University Press.

Scott, W.B. 1941. The mammalian fauna of the White River Oligocene. Part 5. Perissodactyla. Transactions of the American Philosophical Society 28: 747–980.

Sisson, S., J.D. Grossman, and R. Getty. 1975. The anatomy of the domestic animals, 5th ed. Philadelphia: W.B. Saunders Company.

Smith, T., et al. 2015. First early Eocene tapiroid from India and its implication for the paleobiogeographic origin of perissodactyls. Palaeovertebrata 39 ((2)-e5): 1–9.

Sun, B., et al. 2009. Magnetostratigraphy of the Early Paleogene in the Erlian Basin. Journal of Stratigraphy 33: 62–68.

Swofford, D.L. 2002. PAUP*. Phylogenetic analysis using parsimony (*and other methods). Version 4. Sunderland, MA: Sinauer Associates.

Tabrum, A. 2012. Additional material of the type specimen of the tapiroid *Colodon kayi* (Hough) from the Sage Creek Basin, Montana. Abstracts of Papers, Society of Vertebrate Paleontology: 182–183.

Takai, F. 1939. Eocene mammals found from the Hosan coal-field, Tyosen. Journal of the Faculty of Science Tokyo 2 (5): 199–217.

Tokunaga, S. 1933. A list of the fossil land mammals of Japan and Korea: with descriptions of new Eocene forms from Korea. American Museum Novitates 627: 1–7.

Tomida, Y. 1983. A new helaletid tapiroid (Perissodactyla, Mammalia) from the Paleogene of Hokkaido, Japan, and the age of the Urahoro Group. Bulletin of the National Science Museum, Tokyo (C) 9: 151–163.

Tong, Y.S., S.H. Zheng, and Z.D. Qiu. 1995. Cenozoic mammal ages of China. Vertebrate PalAsiatica 33 (4): 290–314.

Vandenberghe, N. et al. 2012. The Paleogene Period. *In* F.M. Gradstein et al. (editors), The geologic time scale 2012, vol. 2: 855–921. Amsterdam: Elsevier.

Wall, W.P., and E. Manning. 1986. *Rostriamynodon grangeri* n. gen., n. sp. of amynodontid (Perissodactyla, Rhinocerotoidea) with comments on the phylogenetic history of Eocene Amynodontidae. Journal of Paleontology 60 (4): 911–919.

Wang, Y.Q., J. Meng, and X. Jin. 2012. Comments on Paleogene localities and stratigraphy in the Erlian Basin, Nei Mongol, China. Vertebrata PalAsiatica 50 (3): 181–203.

Wang, Y.Q., et al. 2010. Early Paleogene stratigraphic sequences, mammalian evolution and its response to environmental changes in Erlian Basin, Inner Mongolia, China. Science China-Earth Sciences 53 (12): 1918–1926.

Wible, J.R. 1983. The internal carotid artery in early eutherians. Acta Palaeontologica Polonica 28 (1–2): 281–293.

Wible, J.R. 1986. Transformations in the extracranial course of the internal carotid artery in mammalian phylogeny. Journal of Vertebrate Paleontology 6 (4): 313–325.

Wible, J.R. 2003. On the cranial osteology of the short-tailed opposum *Monodelphis brevicaudata* (Didelphidae, Marsupialia). Annals of the Carnegie Museum 72: 137–202.

Wilson, J. and J. Schiebout. 1984. Early Tertiary vertebrate faunas, Trans-Pecos Texas: Ceratomorpha less Amynodontidae. Texas Memorial Museum Pearce-Sellards Series 39: 1–47.

Ye, J. 1983. Mammalian fauna from the late Eocene of Ulan Shireh Area, Inner Mongolia. Vertebrata PalAsiatica 21 (2): 109–118.

APPENDIX 1

Taxa and Characters in the Phylogenetic Analyses

The following specimens and references were checked for the coding of the taxa.

Outgroup

Homogalax protapirinus, AMNH FM 4460, 15371, Radinsky (1963)

Ingroup

Heptodon calciculus, AMNH FM 294, 4858, 14884, Radinsky (1963)

Helaletes nanus, AMNH FM 11635, 13124, Radinsky (1963)

Thuliadanta mayri, CMN 30804 (cast AMNH FM 101525), Eberle (2005)

Desmatotherium intermedius, YPM–PU 10166 (cast AMNH FM 10639), AMNH FM 12672, Radinsky (1963), Schoch (1984)

Desmatotherium mongoliense, AMNH FM 19161, 20155, 81718, 81803, IVPP V 14692, Radinsky (1965a)

Paracolodon fissus, AMNH FM 20161, 81802, IVPP V 22640, Radinsky (1965a)

Paracolodon inceptus, AMNH FM 20355, 20357, Radinsky (1965a), Dashzeveg and Hooker (1997)

Colodon? *keyi*, Hough (1955), Radinsky (1963)

Colodon? *woodi*, USNM 20200 (cast AMNH FM 108356), UM 12569, 13943 (cast AMNH FM 108046), Gazin (1956), Radinsky (1963), Eaton (1985)

Plesiocolopirus hancocki, UOMNH 20377 (cast AMNH FM 99380), AMNH FM 99379 (cast), Radinsky (1963)

Hesperaletes, Colbert (2006)

Colodon occidentus, AMNH FM 1212, 9779, F:AM 42891, Radinsky (1963)

Colodon? *cingulatus*, AMNH FM 42897, 42898, 42899, Radinsky (1963)

Colodon stovalli, Wilson and Schiebout (1984)

Colodon orientalis, PIN 1442/99 (cast AMNH FM 21893), Radinsky (1965a)

Dilophodon minusculus, YPM–PU 10019 (cast AMNH FM 10638), AMNH FM 1634a, 13206, Radinsky (1963)

Heteraletes leotanus, CM 11992, AMNH F:AM 104713 (cast), Radinsky (1963)

Protapirus, YPM–PU 10900 (cast AMNH FM 10643), AMNH FM 661, Scott (1941)

Characters

Upper teeth

1. Diastema between canine and incisors: **0,** short; **1,** long.
2. Upper canine: **0,** large; **1,** small; **2,** absent.
3. Postcanine diastema: **0,** short; **1,** long. If the postcanine diastema is shorter or equal to the length of P1–2, it is short (state 0). If the postcanine diastema is longer than the length of P1–2, it is long (state 1).
4. P1 metacone: **0,** absent; **1,** rudimentary; **2,** distinct. Radinsky (1963) interpreted a small cuspule distal to the paracone as the metastyle in *Colodon occidentus* and *Heteraletes leotanus*, but we consider the small cuspule as the metacone, and thus incipiently separated from the paracone.
5. P1 protocone: **0,** absent or very weak; **1,** distinct.
6. P2–4 parastyle: **0,** low; **1,** high.
7. P2 paracone and metacone buccal surface: **0,** convex; **1,** moderately convex and somewhat merged with ectoloph.

8. P2–4 lingual cingulum: **0,** absent; **1,** present.
9. P2 metacone: **0,** smaller than paracone; **2,** as large as paracone.
10. P2 paracone and metacone: **0,** close; **1,** moderately separated; **2,** widely separated. The separation of paracone and metacone is determined by the buccal groove between them. If the paracone and metacone are closely situated (state 0), the groove is rather narrow. If the paracone and metacone are moderately separated (state 1), the groove is relatively wide near the crown but not extended to the base of the crown. If the paracone and metacone are widely separated (state 2), the groove is relatively wide and extended to the base of the crown.
11. P2 hypocone: **0,** absent; **1,** incipient separated from protocone by shallow lingual groove; **2,** distinctly separated from the protocone by a deep lingual groove; **3,** protocone incipient separated by a distinct mesiolingual groove.
12. P2 protoloph: **0,** separated from ectoloph by a notch; **1,** joining the ectoloph.
13. P2 metaloph: **0,** absent; **1,** weak; **2,** as prominent as protoloph.
14. P2 metaloph orientation: **0,** toward protocone; **1,** toward protocone; bypassing hypocone; **2,** toward hypocone.
15. P3–4: **0,** equidimensional or only slightly broader than long; **1,** transversely elongate (from Dashzeveg and Hooker, 1997: char. 18).
16. P3 parastyle separation from paracone: **0,** wide; **1,** narrow.
17. P3 paracone and metacone: **0,** close; **1,** moderately separated; **2,** widely separated.
18. P3 paracone and metacone buccal surface: **0,** convex; **1,** moderately convex and somewhat merged with ectoloph.
19. P3 hypocone: **0,** absent; **1,** protocone distally extended without lingual groove; **2,** incipiently separated from protocone by shallow lingual groove; **3,** distinctly separated from the protocone by a deep lingual groove; **4,** protocone incipient separated by an shallow mesiolingual groove.
20. P3 protoloph: **0,** separated from ectoloph by a notch; **1,** joining the ectoloph.
21. P3 metaloph: **0,** absent; **1,** weak; **2,** as prominent as protoloph.
22. P3 metaloph orientation: **0,** toward protocone; **1,** toward protocone; bypassing hypocone; **2,** toward hypocone.
23. P4 metacone position: **0,** distal to paracone; **1,** more lingually displaced.
24. P4 paracone and metacone: **0,** close; **1,** moderately separated; **2,** widely separated.
25. P4 paracone and metacone buccal surface: **0,** convex; **1,** moderately convex and somewhat merged with ectoloph.
26. P4 hypocone: **0,** absent; **1,** protocone distally extended without lingual groove; **2,** incipiently separated from protocone by shallow lingual groove; **3,** distinctly separated from the protocone by a deep groove; **4,** protocone incipiently separated by a shallow mesiolingual groove; **5,** completely separated.
27. P4 protoloph: **0,** separated from ectoloph by a notch; **1,** joining the ectoloph.
28. P4 metaloph: **0,** weak, not distinct; **1,** as prominent as protoloph.
29. P4 metaloph orientation: **0,** toward protocone; **1,** toward protocone; bypassing hypocone; **2,** toward hypocone.
30. M1–3 parastyle: **0,** separated from paracone; **1,** closely appressed to paracone.
31. M1 metacone buccal surface: **0,** slightly convex; **1,** concave.
32. M1–2 protoloph and metaloph: **0,** straight; **1,** slightly convex mesially.
33. M1–2 metacone: **0,** moderately long; **1,** short; **2,** very reduced.

34. M1–2 metacone position compared with paracone: **0,** slightly lingually depressed; **1,** moderately lingually depressed; **2,** strongly lingually depressed.
35. M1–2 distobuccal cingulum on the buccal side of metacone: **0,** weak; **1,** distinct.
36. M1–2 centrocrista: **0,** directly connecting paracone and metacone; **1,** curved buccally forming reverse U shape.
37. M1–2 metaloph and ectoloph connection: **0,** mesiolingual base of metacone; **1,** near the apex of metacone; **2,** mesial to the apex of the metacone.
38. M2 metacone: **0,** vertically situated; **1,** curved distally at the apex.
39. M2 metacone buccal surface: **0,** slightly convex; **1,** concave.
40. M3 parastyle position compared with paracone: **0,** strongly mesiobuccally; **1,** slightly mesiobuccally; **2,** nearly mesially. Except for *Homogalax* and *Heptodon*, the character state can be determinated by the orientation of preparacrista. The slightly mesiobuccally displaced paracone is indicated by nearly mesially extended preparacrista (state 1). The nearly mesially displaced paracone is indicated by a slightly mesiolingually extended preparacrista (state 2).
41. M3 metacone buccal surface: **0,** slightly convex; **1,** concave.
42. M3 metacone position compared with paracone: **0,** slightly lingually depressed; **1,** moderately lingually depressed; **2,** strongly lingually depressed.
43. Orientation of M3 postmetacrista: **0,** distally; **1,** distobuccally.

Lower teeth

44. Lower canine: **0,** large; **1,** small; **2,** absent.
45. Lower postcanine diastema: **0,** short; **1,** long. The short postcanine diastema refers to the diastema equal to or less than the length of p2–3 (state 0).
46. p1: **0,** present; **1,** absent.
47. p2 metaconid: **0,** absent; **1,** rudimentary; **2,** prominent as protoconid.
48. p2 entoconid: **0,** absent; **1,** weak; **2,** prominent.
49. p2–4 distobuccal cingulum: **0,** present; **1,** absent.
50. p3–4 cristid obliqua orientation: **0,** mesolingually; **1,** mesially toward protoconid.
51. p3 entoconid: **0,** absent; **1,** small and weak; **2,** prominent; **3,** as large as hypocone.
52. p3 protoconid and metaconid: **0,** close; **1,** widely separated.
53. p3 paraconid: **0,** high and prominent; **1,** low and indistinct.
54. p3 trigonid: **0,** longer than wide or equal; **1,** wider than long.
55. p3 talonid width compared with trigonid width: **0,** equal; **1,** slightly greater; **2,** considerably greater.
56. p4 entoconid: **0,** absent; **1,** small and weak; **2,** prominent; **3,** as large as hypocone.
57. p4 trigonid: **0,** longer than wide or equal; **1,** wider than long.
58. p4 talonid width compared with trigonid width: **0,** equal; **1,** slightly greater; **2,** considerably greater.
59. m1–3 paracristid: **0,** distinct; **1,** reduced.
60. m1–3 cristid obliqua: **0,** distinct; **1,** moderately reduced; **2,** highly reduced.
61. m1–3 protolophid and hypolophid: **0,** protolophid transversely extended, hypolophid slightly oblique; **1,** both oblique and parallel to each other; **2,** both transverse.
62. m1–3 endocristid (cristid extending mesially from the entoconid): **0,** present; **1,** absent.
63. m3 hypoconulid: **0,** large; **1,** small; **2,** highly reduced.

Cranium and mandible

64. Position of infraorbital foramen: **0,** posterior border of P2; **1,** posterior border of P3; **2,** posterior end of P4.
65. The posterior end of incisor notch at the level of: **0,** incisors; **1,** postcanine diastema; **2,** P3–4; **3,** M1–2.
66. Anterior end of nasal at the level of: **0,** premaxilla; **1,** postcanine diastema.
67. Premaxilla and nasal contact: **0,** present; **1,** absent.
68. Lateral trough of ascending process of maxilla: **0,** absent; **1,** present.
69. The extension of the lateral trough of ascending process of maxilla: **0,** restrict to the lateral side; **1,** curving around the nasofrontal suture; **2,** extending posteriorly over the supraorbital process of the frontal.
70. The relation between the lacrimal and the lateral border of the lateral trough: **0,** lacrimal narrow and not forming the lateral border; **1,** lacrimal forming part of lateral border.
71. Dorsal surface of frontal: **0,** flat; **1,** with medial trough.
72. Anterior sagittal ridge on the frontal: **0,** absent; **1,** present.
73. Posterior end of symphysis of mandible: **0,** posterior to the first premolar; **1,** anterior to the first premolar; **2,** at the level of the anterior border of the first premolar.

APPENDIX 2

Data Matrix

A = (0/1); B = (0/2); C = (1/2); D = (2/3); E = (0/4).

	1	1	1	1	1	1	1	1	2	2	2	2	2	2	2	2	2	3	3	3	3	3	3	3	3	3
	1	2	3	4	5	6	7	8	9	0	1	2	3	4	5	6	7	8	9	0	1	2	3	4	5	6	7	8	9	0	1	2	3	4	5	6	7	8	9
Homogalax	0	0	0	0	0	0	0	0	0	0	0	0	0	–	0	0	0	0	0	0	0	–	0	1	0	0	0	0	0	0	0	0	0	0	0	0	0	0	0	0
Heptodon	0	0	0	0	0	0	0	0	0	0	0	1	0	–	0	0	0	0	0	1	1	0	0	1	0	0	1	0	0	0	0	0	0	0	0	0	1	0	1
Helaletes	1	1	1	1	0	0	0	0	1	0	A	0	1	0	0	1	0	0	1	1	1	0	1	1	0	C	1	1	0	0	0	0	0	1	0	0	1	0	1
Thuliadanta	?	1	1	0	0	0	1	1	1	0	0	0	0	–	0	0	0	1	1	0	1	0	1	1	1	1	0	0	0	0	1	0	1	1	0	0	1	0	1
Des. intermedius	?	0	1	?	?	0	1	0	1	1	1	0	0	–	0	0	1	1	3	0	1	1	0	1	1	3	1	1	1	1	0	1	0	1	A	0	1	1	1
Des. mongoliense	0	0	1	1	0	1	1	0	1	0	1	0	1	2	0	1	A	1	2	0	1	2	1	0	1	3	1	1	2	1	?	A	1	2	0	0	1	1	1
Pa. fissus	?	?	?	?	?	1	0	0	1	0	D	0	1	1	1	1	0	0	3	0	C	1	1	0	0	3	0	A	1	1	1	0	1	2	1	0	1	0	1
Pa. inceptus	?	?	0	2	1	1	0	0	1	1	2	0	2	2	1	1	1	0	4	0	2	2	1	1	0	2	0	1	0	1	1	0	2	2	1	0	1	0	1
C.? kayi	?	?	?	?	?	?	0	2	?	?	?	?	?	?	1	1	0	0	?	?	2	2	1	0	0	3	0	1	2	1	1	1	1	1	1	0	1	0	1
C.? woodi	?	?	?	0	0	?	0	2	1	0	?	?	?	?	1	1	0	0	3	?	2	2	0	0	0	3	0	1	2	1	1	0	1	1	1	0	1	0	1
Plesiocolopirus	?	1	0	0	0	?	0	0	1	1	3	0	1	0	1	1	0	0	4	1	1	?	1	0	0	4	1	1	0	1	0	0	1	2	0	0	1	0	0
Hesperaletes	1	0	1	0	0	?	1	0	?	?	0	0	A	0	0	1	?	1	?	A	1	0	1	1	1	0	1	0	0	1	0	1	0	1	0	0	2	?	0
C. occidentalis	–	2	1	1	1	1	1	B	1	2	2	0	2	2	1	1	2	1	3	1	2	2	1	2	1	3	1	1	2	1	1	0	2	2	1	1	1	0	1
C.? cingulatus	0	1	0	1	1	1	1	2	1	0	A	0	1	2	1	1	1	1	0	1	2	0	1	1	1	0	1	1	0	1	0	0	0	2	0	1	1	0	0
C. stovalli	?	?	?	?	?	?	0	0	2	1	?	3	?	2	2	1	?	0	0	4	?	2	2	0	0	0	2	1	1	0	1	?	0	1	0	?	1	2	0	?
C. orientalis	?	?	?	?	?	?	?	?	?	?	?	?	?	?	?	?	?	?	?	?	?	?	?	1	2	1	5	1	1	2	1	1	0	2	2	1	1	1	0	1
Dilophodon	?	?	?	?	?	0	1	0	0	?	0	?	1	0	0	?	?	1	E	?	A	0	1	?	1	0	?	0	?	0	1	1	0	1	0	0	2	0	1
Heteraletes	?	?	?	1	0	1	0	2	1	1	0	0	0	–	0	1	1	0	2	0	1	1	0	1	0	2	1	0	1	0	0	1	0	1	0	0	2	0	1
Protapirus	0	1	1	?	?	0	0	0	1	1	0	0	2	0	1	1	2	0	4	1	2	?	1	2	0	2	1	1	0	1	0	1	1	1	0	0	1	0	0

continued

	4	4	4	4	4	4	4	4	4	4	5	5	5	5	5	5	5	5	5	6	6	6	6	6	6	6	6	7	7	7	7
	0	1	2	3	4	5	6	7	8	9	0	1	2	3	4	5	6	7	8	9	0	1	2	3	4	5	6	7	8	9	0	1	2	3
Homogalax	0	0	0	0	0	0	0	0	0	0	0	0	0	0	0	1	1	0	0	0	0	0	0	0	A	0	0	0	0	–	–	0	0	0
Heptodon	1	1	0	1	0	1	A	0	0	0	0	0	0	1	0	0	A	0	0	0	1	1	0	1	1	1	0	0	0	–	–	0	0	0
Helaletes	1	1	1	0	1	1	1	1	0	0	0	1	0	1	0	1	1	0	0	0	2	1	1	1	2	2	0	1	1	0	0	0	0	1
Thuliadanta	2	1	2	0	?	?	0	1	1	?	0	2	0	1	0	1	2	1	1	0	1	?	?	0	2	2	?	1	?	?	?	?	?	?
Des. intermedius	2	0	1	0	?	?	1	1	0	0	1	2	0	1	0	2	2	0	2	0	2	0	1	2	2	?	?	?	?	?	?	?	?	1
Des. mongoliense	2	1	2	1	1	?	1	1	1	0	1	2	0	A	0	1	2	0	1	0	2	0	1	1	2	2	?	1	1	?	0	?	?	1
Pa. fissus	1	1	1	1	?	0	1	A	A	1	1	C	0	0	0	1	C	1	1	0	2	0	?	2	1	?	?	?	1	2	1	1	1	2
Pa. inceptus	1	1	2	1	?	?	?	?	?	?	?	?	?	?	?	?	?	?	?	1	2	0	?	C	?	?	?	?	?	?	?	?	?	?
C.? kayi	1	1	1	1	1	0	1	2	2	0	1	2	1	1	1	2	2	1	2	0	2	2	1	?	?	?	?	?	?	?	?	?	?	?
C.? woodi	2	1	1	1	?	?	?	?	?	0	1	?	?	?	?	?	2	1	1	0	2	1	1	0	?	?	?	?	?	?	?	?	?	?
Plesiocolopirus	2	?	1	0	1	0	1	1	1	0	0	2	0	1	0	1	2	1	2	0	2	1	1	1	1	?	?	1	1	?	?	?	?	1
Hesperaletes	2	0	1	0	0	1	0	1	0	?	1	0	0	1	?	1	1	?	0	0	1	1	1	2	0	2	0	1	1	2	1	1	1	2
C. occidentalis	2	1	1	0	2	–	1	2	2	1	1	3	1	1	1	2	3	1	2	1	2	0	1	1	1	3	1	1	1	1	1	0	0	2
C.? cingulatus	1	0	1	0	1	0	1	2	?	1	1	2	1	1	0	1	2	1	0	1	2	2	?	0	2	2	?	1	1	?	?	0	0	2
C. stovalli	?	?	0	0	1	1	1	1	1	?	1	2	0	1	1	2	3	1	2	1	2	2	?	0	?	2	?	1	1	?	?	?	?	2
C. orientalis	2	1	1	1	?	?	?	?	?	?	?	?	?	?	?	?	?	?	?	?	?	?	?	?	?	?	?	?	?	?	?	?	?	?
Dilophodon	?	?	?	?	1	1	1	0	0	0	1	1	0	1	0	1	1	0	1	0	2	1	1	2	0	?	?	?	0	–	–	0	0	2
Heteraletes	2	1	1	1	?	?	?	?	0	?	1	1	0	1	0	1	1	0	1	0	2	1	1	2	?	?	?	?	?	?	?	?	?	?
Protapirus	1	0	1	0	1	1	1	2	2	1	0	2	1	1	1	1	2	1	1	1	2	C	1	2	1	2	1	1	1	2	1	1	1	2

APPENDIX 3

Distribution of Unambiguous Synapomorphies (tree, fig. 11).

Numbers in parentheses correspond to character states; "-" precedes reversal characters. Nonhomoplastic synapomorphies are in bold; other characters are homoplastic.

Node	Characters and state
35	3(1), 7(1), 16(1), 18(1), 23(1), 25(1), 32(1), 34(1), 42(1), 50(1), **62(1)**, **67(1)**, 73(2)
34	**44(1)**, 46(1), 58(1), 60(2)
33	**9(1)**, 26(2), 64(2), -73(1)
32	4(1), 17(1), 22(1), 29(1)
31	11(1), 26(3), 28(1), 30(1), **38(1)**, -61(0)
30	**2(1)**, -32(0), -50(0)
29	-7(0), 13(1), -18(0), 20(1), -25(0), 28(1),
28	**15(1)**, 19(4), -24(0), 30(1), -64(1)
27	13(2), **21(2)**, 49(1), 59(1), 73(2)
26	14(2), 31(1), 35(1), 50(1)
25	8(1), 55(2), 58(2), -63(0)
24	-19(3), 26(3), 47(2), 48(2), 52(1)
23	4(1), 7(1), 18(1), 25(1),
22	40(2)
21	-27(0), 43(1), -49(0), -59(0),
20	-20(0), -27(0), 43(1)

All issues of *Novitates* and *Bulletin* are available on the web (http://digitallibrary.amnh.org/dspace). Order printed copies on the web from:
http://shop.amnh.org/a701/shop-by-category/books/scientific-publications.html

or via standard mail from:

American Museum of Natural History—Scientific Publications
Central Park West at 79th Street
New York, NY 10024

♾ This paper meets the requirements of ANSI/NISO Z39.48-1992 (permanence of paper).